

High Dimensional Model Representation as a Glass Box in Supervised Machine Learning

Caleb Deen Bastian, Herschel Rabitz

July 30, 2018

Abstract

Prediction and explanation are key objects in supervised machine learning, where predictive models are known as black boxes and explanatory models are known as glass boxes. Explanation provides the necessary and sufficient information to interpret the model output in terms of the model input. It includes assessments of model output dependence on important input variables and measures of input variable importance to model output. High dimensional model representation (HDMR), also known as the generalized functional ANOVA expansion, provides useful insight into the input-output behavior of supervised machine learning models. This article gives applications of HDMR in supervised machine learning. The first application is characterizing information leakage in “big-data” settings. The second application is reduced-order representation of elementary symmetric polynomials. The third application is analysis of variance with correlated variables. The last application is estimation of HDMR from kernel machine and decision tree black box representations. These results suggest HDMR to have broad utility within machine learning as a glass box representation.

Contents

1	Introduction	2
1.1	Motivations of representation	2
1.2	Related work	3
1.3	Contributions	4
1.4	Organization	4
2	Preliminaries	5
3	High dimensional model representation	6
3.1	Eliminating information leakage in “big-data” settings	8
3.2	Reduced-order representation of high-dimensional behavior	11
3.3	Analysis of variance for correlated input variables	14

4	Interpretative diagnostics	18
4.1	Partial dependence	18
4.2	Derivative-based global sensitivity measures	19
4.3	Illustration	19
5	Glass boxes from black boxes	23
5.1	Kernel machines	23
5.2	Decision trees	26
6	Concluding Remarks	37
	Appendices	38

1 Introduction

In many areas of science and engineering one is typically interested in using empirical data \mathbf{D} to understand an input-output map f from some class of systems F , often having a large number of input and output variables. We indicate the input space by (X, \mathcal{X}) , the output space by (Y, \mathcal{Y}) , and the system (model) space as $F = Y^X$, and put $n \equiv |X| \in \mathbb{N}$ and $p \equiv |Y| \in \mathbb{N}$ respectively. Suppose \mathbf{D} is a collection of *iid* random variables taking values in $X \times Y$, denoted by $\mathbf{D} = \{(x_i, y_i)\}$, and regard each (x_i, y_i) as a realization from the probability measure ν .

This setting can be identified to *supervised machine learning* [Vapnik, 1995], where f is a prediction function, F is some class of candidate functions, and ν is the joint probability measure on $X \times Y$ whose independent random realizations form \mathbf{D} . The task for supervised machine learning is solving

$$f^* = \arg \min_{f \in F} R(f),$$

where R is a risk functional

$$R : f \mapsto \frac{1}{N} \sum_{(x,y) \in \mathbf{D}} L(y, f(x))$$

with sample size $N \in \mathbb{N}$ and where L is a loss function, $L : X \times Y \mapsto \mathbb{R}_+$. The learned f^* is used to assign an element $f^*(x)$ of Y to each x in X . In this article we consider quadratic loss function $L(y, f(x)) = (y - f(x))^2$.

1.1 Motivations of representation

The input-output relation f can be represented many ways. *Black box* representation is solely concerned with the task of assigning an element $f(x)$ of Y to each x in X (*prediction*) and includes all such functions from X into Y . In other words, the particular structure

of f is irrelevant so long as it is contained in F , and notions of input variable importance and dependence of f upon the important variables are abstract. General-purpose black box learning algorithms in machine learning include neural networks, kernel machines, and decision tree models. *Glass box* representation restricts F to include only those functions which provide information on variable importance and dependence (*explanation*). Glass box representation means that F is equipped with necessary and sufficient information to interpret the model output in terms of the model input. This information is referred to as *interpretative diagnostics* and is defined by the variable importance and variable dependence sets $I(f)$ and $P(f)$ respectively, each indexed on $\mathcal{P}(\{1, \dots, n\})$. Hooker [2007] discusses diagnostics for high-dimensional functions based upon projection operators, and functionals can be further defined to measure variable importance from projections. These ideas are adopted in this article to construct $I(f)$ and $P(f)$.

A consideration is managing the sizes of $I(f)$ and $P(f)$ as the number of input variables increases, each of size 2^n . The exponential growth is known as the *curse of dimensionality*. For large enough n , construction cost outstrips available resources, and feasibility is achieved through simplifying assumptions on F or μ , e.g., stipulating restrictions on model form or distribution. A large body of work supports the *ansatz* that many high-dimensional systems especially those of a physical (or real-world) nature are accurately, if not exactly, described by representations whose sizes grow polynomially in n .

The *ansatz* is elevated to theorem in a result of Kolmogorov [Lorentz et al., 1996]: his superposition theorem, an existence result, establishes that every multivariate continuous function on the unit cube $X = [0, 1]^n$ can be exactly represented using a finite number of univariate continuous functions and the binary operation of addition,

$$f(x) = \sum_{i=1}^{2n+1} \phi_i \circ \left(\sum_{j=1}^n \psi_{ij} \circ x_j \right),$$

where ϕ_i are ψ_{ij} are continuous functions. These functions are highly non-smooth, limiting their utility in approximation.

Instead of seeking a representation in terms of univariate functions, suppose a hierarchy of projections into subspaces of increasing dimensions, with the expectation that subspace contributions to output(s) rapidly diminish with increasing dimension. This is the idea behind a mathematical model called *high dimensional model representation* (HDMR), a finite multivariate representation that efficiently manages the curse of dimensionality and that provides structured information for input-output relationships. When applied to supervised machine learning models, HDMR is a glass box that interprets the model output in terms of the model input.

1.2 Related work

HDMR is discussed as early as Fisher [1921] in ANOVA analysis and has enjoyed extensive application to statistics. When F is the collection of symmetric functionals of *iid* variables

HDMR is known as the Hoeffding decomposition, a fundamental object in U-statistics [Hoeffding, 1948]. The univariate terms of HDMR are sometimes known as Hajek projections and are extensively used to establish asymptotic normality of various statistics [Hajek, 1968]. Global sensitivity analysis (GSA) measures the importance of variables to F [Sobol, 2001, 1990, I.M. Sobol, 2004]. In GSA applications functional representation of F is avoided where instead sensitivity indices are directly estimated. [Rabitz and Alis, 1999] discussed HDMR as a general decomposition of F where the input space resides in \mathbb{R}^n or in the n -fold product space of arbitrary linear topological function spaces. These ideas have been further developed to F for general (non-degenerate) distributions in Hooker [2007], wherein HDMR is known as generalized functional ANOVA, which in turn provisions GSA in terms of structural and relative sensitivity indices [Li and Rabitz, 2012]. Sometimes HDMR is known as the Hoeffding-Sobol decomposition [Chastaing et al., 2012] or Sobol decomposition [Arwade et al., 2010]. See Takemura [1983] for references on HDMR’s earlier history.

1.3 Contributions

We discuss HDMR and provide illustrative applications to motivate its utility to supervised machine learning. First, we illustrate that HDMR can diagnose information leakage. This is demonstrated for Pearson goodness-of-fit settings for “big-data” wherein HDMR characterizes estimator efficiency loss and for popular machine learning black boxes wherein HDMR identifies biases. Second, we illustrate that HDMR characterizes the information leakage experienced by partial dependence, another interpretative diagnostic, whenever input variables are correlated. In such settings, HDMR reveals that the interpretative diagnostics functionally depend upon the distribution correlation. Third, we demonstrate that HDMR admits efficient reduced-order representations of high-dimensional models, managing the curse of dimensionality. In particular, we illustrate that the input distribution regulates the efficiency of reduced-order representation in polynomials and demonstrate this effect in a learning setting. Fourth, we demonstrate that HDMR can be applied as a wrapper method for black boxes to provision glass boxes. Fifth, we estimate HDMR of trained kernel machines or ensembles of decision trees.

1.4 Organization

In section 2 we formulate interpretative diagnostics using projection operators and functionals and related quantities. In section 3 we discuss HDMR and provide three examples of applications: (i) to goodness-of-fit in “big-data” settings (subsection 3.1), (ii) high-dimensional modeling (subsection 3.2), and (iii) analysis of variance (subsection 3.3). In section 4 we consider alternative interpretative diagnostics and compare to HDMR for a simple mathematical model having an analytic solution. In section 5 we apply HDMR as a wrapper method for black boxes to convey information on variable importance and

dependence, and we consider two machine learning black boxes—kernel machines (subsection 5.1) and decision trees (subsection 5.2)—on analytic and empirical (test dataset) problems. We conclude with a discussion.

2 Preliminaries

In this article we consider the model space to be square-integrable functions $F = L^2(X, \mathcal{X}, \mu)$. We formulate interpretative diagnostics for the subspaces $u \subseteq \{1, \dots, n\}$ (*notationally we use $\mathbb{N}_n = \{1, \dots, n\}$ throughout this article*) using projection operators and functionals. For every $u \subseteq \mathbb{N}_n$ let \mathbf{P}^u be a projection operator that profiles the dependence of f on x_u and put $f_u \equiv \mathbf{P}^u f$; f_u is said to be the *variable dependence* or projection of f on x_u . Let $\mathbf{I}^u : F \mapsto \mathbb{R}_+$ be a functional that measures the importance of $f \in F$ on x_u and put $S_u \equiv \mathbf{I}^u f$; S_u is said to be a measure of *variable importance* of f on x_u . Using $\{\mathbf{I}^u\}$ and $\{\mathbf{P}^u\}$, we define respective variable importance and variable dependence sets $\mathbf{I}(f) \equiv \{\mathbf{I}^u f\}$ and $\mathbf{P}(f) \equiv \{\mathbf{P}^u f\}$ on $\mathcal{P}(\mathbb{N}_n)$.

Sometimes total and relative notions of variable importance are necessary. We define the *total variable importance* of f on x_i as $T_i \equiv \mathbf{T}^i f$ where $\mathbf{T}^i \equiv \sum_{u \supseteq i} \mathbf{I}^u$. We define the *relative variable importance* of f on x_i as $R_i \equiv \mathbf{R}^i f$ where $\mathbf{R}^i f \equiv \mathbf{T}^i f / \sum_j \mathbf{T}^j f$. Using $\{\mathbf{T}^i\}$ and $\{\mathbf{R}^i\}$ we define total variable importance and relative variable importance sets $\mathbf{T}(f) = \{\mathbf{T}^i f\}$ and $\mathbf{R}(f) = \{\mathbf{R}^i f\}$.

Using $\mathbf{I}(f)$, $\mathbf{P}(f)$, $\mathbf{T}(f)$, and $\mathbf{R}(f)$, we can pose various questions for f as super level-sets:

- (i) which variables are important overall?

$$\mathbf{T}_\epsilon(f) = \{T_i \in \mathbf{T}(f) : T_i \geq \epsilon\}$$

- (ii) what are the relative importances of the variables?

$$\mathbf{R}_\epsilon(f) = \{R_i \in \mathbf{R}(f) : R_i \geq \epsilon\}.$$

- (iii) which variables are important individually?

$$\mathbf{I}_\epsilon(f) = \{S_u \in \mathbf{I}(f) : S_u \geq \epsilon, |u| = 1\}$$

- (iv) which variables participate in interactions?

$$\mathbf{X}_\epsilon(f) = \{S_u \in \mathbf{I}(f) : S_u \geq \epsilon, |u| > 1\}$$

- (v) how does the system depend upon the important variables and interactions?

$$\mathbf{P}_\epsilon(f) = \{f_u \in \mathbf{P}(f) : \mathbf{I}(f) \ni S_u \geq \epsilon\}$$

- (vi) does the system admit a reduced order representation?

$$\exists T \in \{1, \dots, n\} : f \simeq f^T = \sum_{u:|u| \leq T} f_u$$

3 High dimensional model representation

Writing $F = L^2(X, \mathcal{X}, \nu)$, the HDMR of $f(x) \in F$ is the solution to the variational problem

$$\min_u \|f(x) - u\|, \quad u \in \mathcal{V}_0 \oplus \sum_i \mathcal{V}_i \oplus \sum_{i_1 < i_2} \mathcal{V}_{i_1 i_2} \oplus \dots \oplus \sum_{i_1 < \dots < i_l} \mathcal{V}_{i_1 \dots i_l},$$

where the norm $\|\cdot\|$ is induced by the inner product as $\|\cdot\| = \langle \cdot, \cdot \rangle^{1/2}$ and the $\{\mathcal{V}_u \subset F : |u| \leq l\}$ are subspaces having certain null integral properties. It is uniquely minimized by

$$u = \left(\mathcal{P}_0 + \sum_i \mathcal{P}_i + \sum_{i_1 < i_2} \mathcal{P}_{i_1 i_2} + \dots + \sum_{i_1 < \dots < i_l} \mathcal{P}_{i_1 \dots i_l} \right) f(x)$$

using the collection of non-orthogonal projection operators $\{\mathcal{P}_u\}$. Putting

$$\varepsilon_l(x) \equiv f(x) - u = f(x) - f_0 - \sum_i f_i(x_i) - \sum_{i_1 < i_2} f_{i_1 i_2}(x_{i_1}, x_{i_2}) - \dots - \sum_{i_1 < \dots < i_l} f_{i_1 \dots i_l}(x_{i_1}, \dots, x_{i_l}),$$

we express

$$\|f(x) - u\| = \langle \varepsilon_l, \varepsilon_l \rangle^{1/2},$$

which for scalar valued functions is

$$\|f(x) - u\| = \int_X \varepsilon_l^2(x) d\nu(x).$$

The HDMR of $f \in F$ is written as

$$f(x) = f_0 + \sum_i f_i(x_i) + \sum_{i_1 < i_2} f_{i_1 i_2}(x_{i_1}, x_{i_2}) + \dots + f_{1 \dots n}(x_1, \dots, x_n),$$

, a sum of 2^n *component functions* [Rabitz and Alis, 1999, Hooker, 2007]. Although many additional component functions appear when compared to Kolmogorov's result, most of these are identically zero or insignificant for many F of practical interest: it is often observed

$$f(x) \simeq f^T(x) = f_0 + \sum_i f_i(x_i) + \sum_{i_1 < i_2} f_{i_1 i_2}(x_{i_1}, x_{i_2}) + \dots + \sum_{i_1 < \dots < i_T} f_{i_1 \dots i_T}(x_{i_1}, \dots, x_{i_T})$$

for $T \ll n$, i.e. f^T is a *reduced-order representation* of f . Whenever $T < n$ and $f(x) \simeq f^T(x)$, we achieve a polynomial-scaling representation in n . In most applications $T \leq 3$ is sufficient. In general, HDMR is expected to exhibit favorable convergence in T whenever the input variables are meaningfully defined in relation to the output variable(s), typically the case with physical systems where input and output variables correspond to observable physical states. Some properties of HDMR:

- (i) it is unique given μ
- (ii) $\{\mathcal{V}_u\}$ are hierarchically orthogonal and partition variance, $\text{Var}(f) = \sum_{u,v} \text{Cov}(f_u, f_v)$
- (iii) $\{\mathcal{V}_u\}$ maximize explained variance, i.e. no other hierarchically-orthogonal functions achieve higher explanatory variance than those belonging to $\{\mathcal{V}_u\}$
- (iv) the elements of $\{\mathcal{V}_u\}$ can be attained through the action of projection operators $\{\mathcal{P}_u\}$ such that $f_u(x_u) \equiv \mathcal{P}_u f(x)$, i.e. the component functions are L^2 projections of $f(x)$
- (v) all HDMR's converge at the same order: if $f^T(x)$ converges for μ with error $\mathcal{O}(\epsilon)$, then $f^T(x)$ converges for μ' with error $\mathcal{O}(\epsilon)$, although the constant can be substantially different
- (vi) for a set of functions $\{f^i(x)\}$ obeying linear-superposition conservation laws, the corresponding HDMR's obey such for every T .

The notion of hierarchical-orthogonality guarantees the existence and uniqueness of the decomposition such that $\text{Var}(f) = \sum_{u,v} \text{Cov}(f_u, f_v)$ [Hooker, 2007]. Note that hierarchical-orthogonality is a generalization of mutual orthogonality where functions are orthogonal only to functions on nested subspaces. For example, for $\mu_{123} \neq \mu_1\mu_2\mu_3$, hierarchical-orthogonality implies $\langle f_{12}, f_1 \rangle = \langle f_{12}, f_2 \rangle = 0$ but neither implies $\langle f_1, f_2 \rangle = 0$ nor $\langle f_{12}, f_3 \rangle = 0$.

Given the variance decomposition, sensitivity indices can be defined in terms of normalized variances and covariances. This is known as *structural and correlative sensitivity analysis* (SCSA) [Li and Rabitz, 2012], where SCSA defines structural, correlative, and overall sensitivity indices ($\mathbb{S}_u^a, \mathbb{S}_u^b, \mathbb{S}_u$) for each component function $u \subseteq \mathbb{N}_n$,

$$\begin{aligned}\mathbb{S}_u^a &\equiv \frac{1}{\text{Var}(f)} \text{Var}(f_u) \\ \mathbb{S}_u^b &\equiv \frac{1}{\text{Var}(f)} \sum_{v:v \neq u} \text{Cov}(f_u, f_v) \\ \mathbb{S}_u &\equiv \mathbb{S}_u^a + \mathbb{S}_u^b,\end{aligned}$$

and these satisfy

$$\sum_u \mathbb{S}_u = 1.$$

Note that when $\mu \neq \prod_i \mu_i$, the projections $f_u = \mathcal{P}_u f$ are hierarchically-orthogonal with $\sum_u \mathbb{S}_u^a < 1$ and $\sum_u (\mathbb{S}_u^a + \mathbb{S}_u^b) = 1$.

When the input variables are independent, $\mu = \prod_i \mu_i$, the component functions are mutually orthogonal and can be recursively constructed,

$$\begin{aligned}
f_{i_1 \dots i_l}(x_{i_1}, \dots, x_{i_l}) &\equiv \mathbf{M}^{i_1 \dots i_l} f(x) - \sum_{j_1 < \dots < j_{l-1} \subset \{i_1, \dots, i_l\}} f_{j_1 \dots j_{l-1}}(x_{j_1}, \dots, x_{j_{l-1}}) \\
&- \sum_{j_1 < \dots < j_{l-2} \subset \{i_1, \dots, i_l\}} f_{j_1 \dots j_{l-2}}(x_{j_1}, \dots, x_{j_{l-2}}) - \dots \\
&- \sum_{j \subset \{i_1, \dots, i_l\}} f_j(x_j) - f_0
\end{aligned} \tag{1}$$

where $\mathbf{M}^{i_1 \dots i_l} f(x) \equiv \int_{X_{-i_1 \dots i_l}} f(x) \prod_{j \notin \{i_1, \dots, i_l\}} d\mu_j(x_j)$ (note that (1) does not hold for correlated μ). Because of the mutual orthogonality of the component functions, we have $\text{Cov}(f_u, f_v) = 0$ for $u \neq v$ such that $\sum_u \mathbb{S}_u^a = 1$. This is known as global sensitivity analysis (GSA) Sobol [1990].

In regard to the projection operators $\{\mathbf{P}^u\}$ and functionals $\{\mathbf{I}^u\}$ of *interpretative diagnostics*, we put for every u

$$\mathbf{P}_{\text{HDMR}}^u f(x) \equiv \mathcal{P}_u f(x) = f_u^{\text{HDMR}}(x_u)$$

and

$$\mathbf{I}_{\text{HDMR}}^u f(x) \equiv (\mathbb{S}_u^a, \mathbb{S}_u^b, \mathbb{S}_u).$$

We provide three examples of HDMR in machine learning.

3.1 Eliminating information leakage in “big-data” settings

Consider an independency of iid random variables $\mathbf{D} = \{X_i\}$ with distribution μ on X . Suppose (X, \mathcal{X}) is discrete and that \mathbf{D} is represented as an infinite double-array $[X_{nj}]$ of real-valued random variables (that is, for each $n \in \mathbb{N}$ there is a $k_n \in \mathbb{N}$ such that $X_{nj} = 0$ for all $j > k_n$). The probability law of X_n is given by $\mu_n\{k\} \equiv \mathbb{P}(X_n = k)$ for $k \in \{1, \dots, k_n\}$. We consider “big-data” to be the case of $k_n \rightarrow \infty$ as $n \rightarrow \infty$, i.e., the dimension of X_n (denoted by k_n) increases to infinity as the sample size (denoted by n) increases so. Consider the goodness-of-fit Pearson chi-square (PGOF) statistic χ_n^2 . For fixed $k_n = k$ the statistic χ_n^2 asymptotically follows the χ^2 -distribution with $(k-1)$ degrees of freedom and whenever k is large the standardized statistic $(\chi_n^2 - (k-1))/\sqrt{2(k-1)}$ is approximated by the standard Gaussian distribution. However, $k_n = k$ is not the case in “big-data” applications where $k_n \rightarrow \infty$ is observed as $n \rightarrow \infty$. As shown in Rempala and Wesolowski [2016] the Gaussian approximation may or may not be valid for the doubly infinite case; furthermore it turns out that the asymptotic behavior of χ_n^2 is characterized

by a subset of its HDMR component functions. Employing the material in the appendices, we define a new statistic using this subset of component functions, denoted by $\chi_{n\text{HDMR}}^2$,

$$\begin{aligned}\chi_{n\text{HDMR}}^2(x_1, \dots, x_n) &\equiv f_0 + \sum_{i < j} f_{ij}(x_i, x_j) \\ &\equiv \chi_n^2(x) - \sum_i f_i(x_i),\end{aligned}$$

and compare its relative efficiency to χ_n^2 for the power law distribution,

$$\alpha \in [0, 1), \quad \mu_n\{k\} = (C_\alpha k^\alpha)^{-1},$$

where

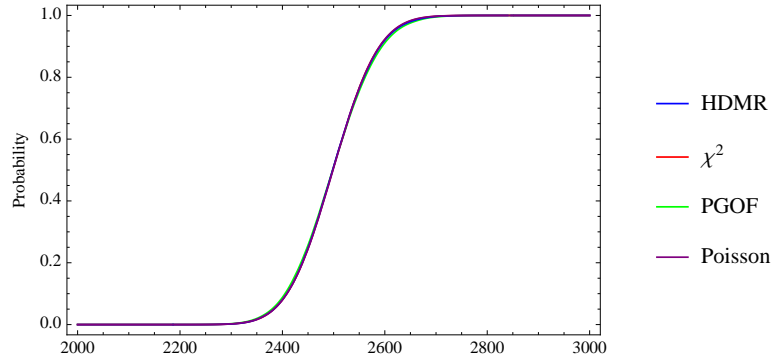
$$C_\alpha = \sum_{k \in [k_n]} k^{-\alpha} \simeq k_n^{1-\alpha} / (1 - \alpha).$$

The HDMR statistic dominates the PGOF statistic.

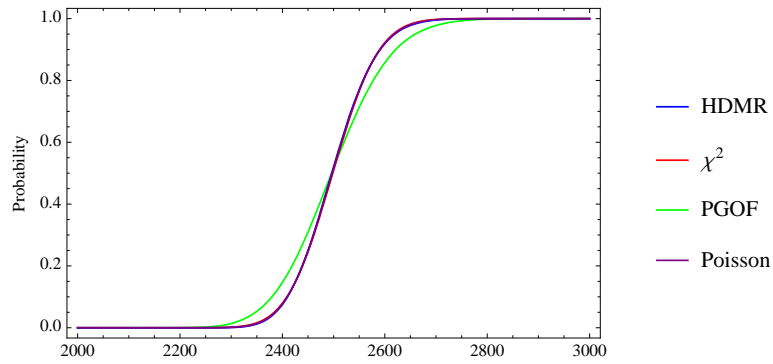
In Figure 1, we exhibit empirical distributions for PGOF, HDMR chi-square, and chi-square for $k_n = 2500$ and $n \in \{50, 500, 5000\}$, having corresponding $\lambda \in \{1, 10, 100\}$, for the power law distribution with $\alpha = 1/2$. We show statistics for the estimators in Table 1. For $\lambda = 100$, Figure 1a shows both χ_n^2 and $\chi_{n\text{HDMR}}^2$ are asymptotically χ^2 . For $\lambda = 10$, Figure 1b shows that χ_n^2 is not asymptotically χ^2 but $\chi_{n\text{HDMR}}^2$ is. For $\lambda = 1$, Figure 1c shows that neither χ_n^2 nor $\chi_{n\text{HDMR}}^2$ is asymptotically χ^2 . In particular, $\chi_{n\text{HDMR}}^2$ is expressed in terms of a Poisson law (see appendices for a precise characterization), although observe that the empirical distribution is truncated due to undersampling of the power law tails. **The HDMR statistic** $\chi_{n\text{HDMR}}^2$ dominates the PGOF statistic χ_n^2 , i.e. PGOF experiences *information leakage* in comparison to the HDMR. For $\lambda = 1$ we observe PGOF to have a relative efficiency of $\sim 10\%$ to that of HDMR.

Table 1: Estimator statistics from 5×10^4 simulations for $k_n = 2500$ and power law distribution with $\alpha = 1/2$

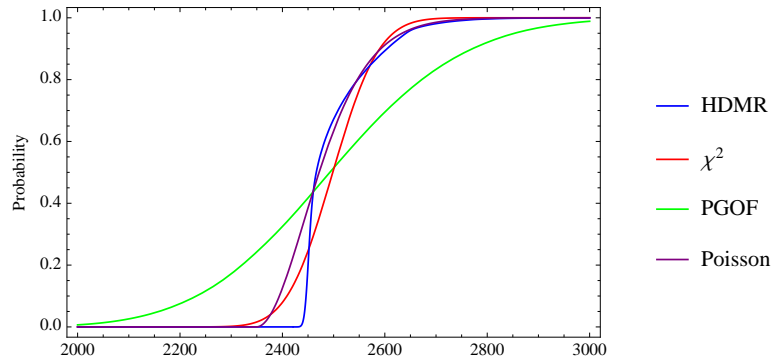
n	k_n	$\lambda \equiv \frac{n}{\sqrt{k_n}}$	\mathbb{E}		Var	
			χ_n^2	$\chi_{n\text{HDMR}}^2$	χ_n^2	$\chi_{n\text{HDMR}}^2$
5000	2500	100	2499.20	2499.18	5464.45	5054.05
500	2500	10	2498.84	2498.83	9023.85	5032.56
50	2500	1	2499.30	2499.45	44188.40	5014.13



(a) $n = 5000$ ($\lambda = 100$)



(b) $n = 500$ ($\lambda = 10$)



(c) $n = 50$ ($\lambda = 1$)

Figure 1: Empirical distributions for $k_n = 2500$ and power law distribution with $\alpha = 1/2$

3.2 Reduced-order representation of high-dimensional behavior

Note that in this section we use ν to indicate the measure on X , and μ and σ denote the mean and standard deviation common to the input variables.

In this application we compute HDMR for polynomial models, in particular the function $\prod_{i=1}^n x_i$ and a sum of elementary symmetric polynomials in n variables. We show that the coefficient of variation ρ of the input distribution ν regulates the efficiency of low-dimensional HDMR approximations. We illustrate these properties for polynomial models.

Consider

$$f(x) = \prod_{i=1}^n x_i, \quad \text{iid } x, \quad \rho \equiv \sigma/\mu \neq 0$$

with

$$\text{Var } f = \mu^{2n} ((1 + \rho^2)^n - 1).$$

Per (1) the component functions of $f(x)$ are

$$\begin{aligned} f_0 &= \mathcal{P}_0 f(x) = \mu^n \\ f_i(x_i) &= \mathcal{P}_i f(x) = \mu^{n-1} x_i - f_0 \\ f_{ij}(x_i, x_j) &= \mathcal{P}_{ij} f(x) = \mu^{n-2} x_i x_j - f_i(x_i) - f_j(x_j) - f_0 \\ &\vdots \end{aligned}$$

Employing the material in the appendices, the sensitivity indices satisfy

$$\sum_{\substack{k \\ i_1 < \dots < i_k}} \mathbb{S}_{i_1 \dots i_k} = 1$$

and at each order follow

$$p\{k\} \equiv \sum_{i_1 < \dots < i_k} \mathbb{S}_{i_1 \dots i_k} = \frac{\binom{n}{k} \rho^{2k}}{(\rho^2 + 1)^n - 1}$$

where $\sum_k p\{k\} = 1$. We have $\mathbb{E} p = \frac{n\rho^2(\rho^2+1)^{n-1}}{(\rho^2+1)^n - 1}$ and $\text{Var } p = \frac{n\rho^2(\rho^2+1)^{n-2}((\rho^2+1)^n - n\rho^2 - 1)}{((\rho^2+1)^n - 1)^2}$.

Observe that when $\rho < 1$ the explained variance of low dimensional approximations increases. For context, the uniform distribution on the unit interval (maximum entropy on $[a, b]$) has $\rho(\text{Unif}[0, 1]) = \frac{\sqrt{3}}{3} \approx 0.58$. In Figure 2, we plot the percent of explained variance by subspace order $\mathbf{p} \equiv (p\{k\} : k \in \mathbb{N}_n)$ for $n = 100$ and $\rho \in \{\frac{1}{4}, \frac{1}{2}, 1, 2, 4\}$. We observe that for $\rho < 1$ the probability mass of the probability vector \mathbf{p} is concentrated

about small k . Similar results are observed for sums of elementary symmetric polynomials in n variables

$$E_n(x) = 1 + \sum_{\substack{k \in \mathbb{N}_n \\ i_1 < \dots < i_k}} x_{i_1} \cdots x_{i_k},$$

where $\tau \equiv \frac{\sigma}{1+\mu}$ regulates efficiency, and are contained in the appendices.

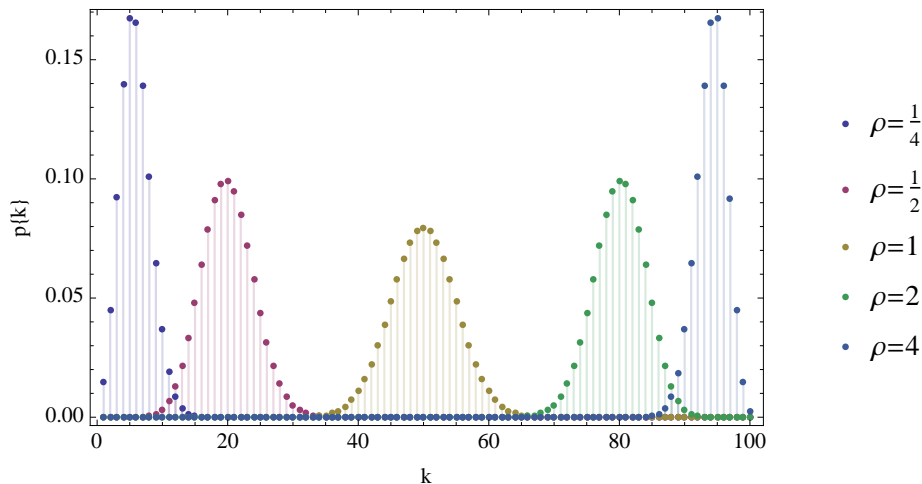
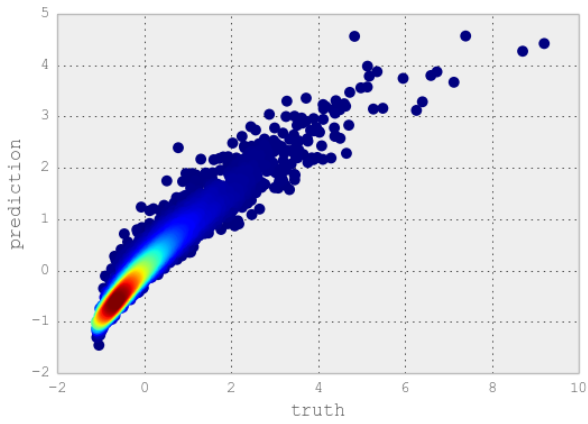
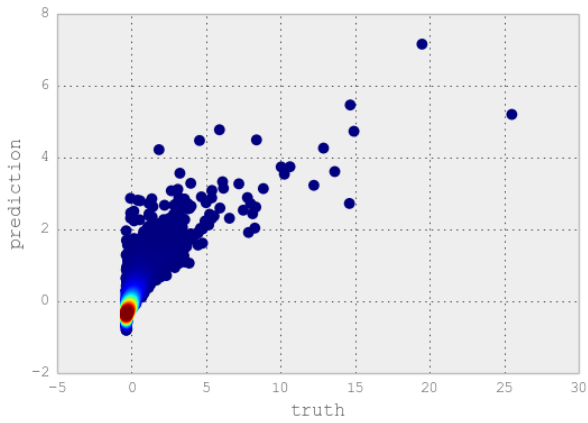


Figure 2: $p\{k\} = \sum_{i_1 < \dots < i_k} S_{i_1 \dots i_k}$

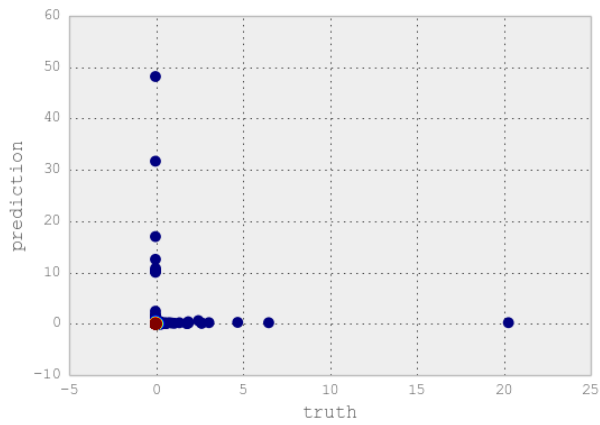
We demonstrate this effect through Monte Carlo estimation of mean-squared-error test performance using the gradient boosting regressor (GBR) machine (Monte Carlo cross-validation), i.e. the generalization ability of the learning algorithm. We take $n = 10$ and form $\mathbf{D} = \{(x_i, f(x_i))\}_{i=1}^{10^4}$ from *iid* random variables from a Beta(a, b) distribution on $X = [0, 1]^n$. For the beta distribution, we take $\rho \in \{\frac{1}{4}, \frac{1}{2}, 1\}$ using $(a, b) \in \{(\frac{15}{2}, \frac{15}{2}), (\frac{3}{2}, \frac{3}{2}), (\frac{1}{2}, \frac{3}{2})\}$. We take a tree depth of six with 5×10^3 trees. We split the data into training and test data. This is performed for 50 independent estimates, where (\mathbf{D}_i) are independently standardized using training data. Mean and standard deviation Monte Carlo estimates are shown below in Table 2 and density truth plots in Figure 3 (inverse-transformed): MSE markedly increases as ρ increases.



(a) $\rho = \frac{1}{4}$



(b) $\rho = \frac{1}{2}$



(c) $\rho = 1$

Figure 3: Density truth plots for test data for $\rho \in \{\frac{1}{4}, \frac{1}{2}, 1\}$

Table 2: Monte Carlo MSE mean and standard deviation in p

ρ	Mean	Std
1/4	0.1207	0.0145
1/2	0.3866	0.1160
1	10.1248	45.55

The total variable importance of x_i to f is computed as

$$T_i = \sum_k \frac{\rho^{2i} \binom{n-1}{k-1}}{(\rho^2 + 1)^n - 1} = \frac{\rho^2}{\rho^2 + 1} \frac{(\rho^2 + 1)^n}{(\rho^2 + 1)^n - 1} \approx \frac{\rho^2}{\rho^2 + 1}.$$

Observe that T_i is independent of the value of n whenever $n > k$ for sufficiently large k . This is depicted in Figure 4 and observed for $k \sim 100$. Relative variable importance is trivially $R_i = n^{-1}$ and is independent of ρ .

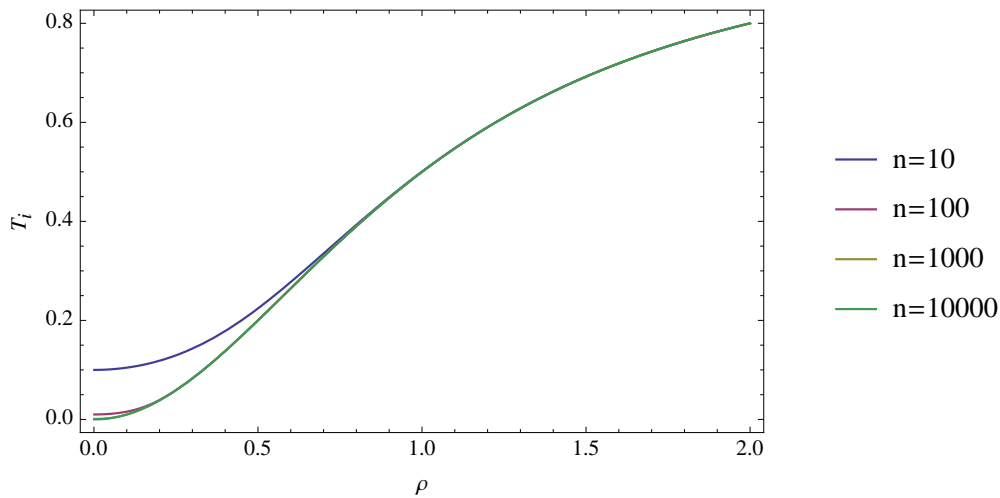


Figure 4: T_i for $(n, \rho) \in \{10, 100, 1000, 10000\} \times [10^{-4}, 1]$

3.3 Analysis of variance for correlated input variables

Note that in this section and subsequent sections, we use μ to indicate the probability measure on (X, \mathcal{X}) .

In this application we show how **variable importance** $\mathbf{I}(f)$ and **variable dependence** $\mathbf{P}(f)$ by **HDMR** depend upon correlation ρ in the input variables and **this is necessary to preserve model variance**. This provisions an analysis of variance that is consistent for correlated or degenerate input variables: total variance is preserved for all values of ρ .

Let

$$F = L^2(\mathbb{R}^n, \mathcal{B}(\mathbb{R}^n), \mu) = \Pi^n \equiv \text{Span}\{x^\alpha : |\alpha| \leq n, \alpha \in \mathbb{N}_0^n\}$$

where $\alpha = (\alpha_1, \dots)$, $|\alpha| = \sum_i \alpha_i$, and μ is Gaussian. In particular, take $n = 2$ and let

$$f(x) = \beta_0 + \beta_1 x_1 + \beta_2 x_2 + \beta_{12} x_1 x_2. \quad (2)$$

Its projections $\{f_u \leftarrow \mathcal{P}_u f\}$ decompose f ,

$$f(x) = f_0 + f_1(x_1) + f_2(x_2) + f_{12}(x_1, x_2),$$

where

$$\begin{aligned} f_0 &= \beta_0 + \beta_1 \mu_1 + \beta_2 \mu_2 + \beta_{12} \mu_1 \mu_2 + \beta_{12} \rho \sigma_1 \sigma_2 \\ f_1(x_1) &= (x_1 - \mu_1)(\beta_1 + \beta_{12} \mu_2) + \left(\frac{\rho}{\rho^2 + 1}\right) \frac{\beta_{12} \sigma_2}{\sigma_1} ((x_1 - \mu_1)^2 - \sigma_1^2) \\ f_2(x_2) &= (x_2 - \mu_2)(\beta_2 + \beta_{12} \mu_1) + \left(\frac{\rho}{\rho^2 + 1}\right) \frac{\beta_{12} \sigma_1}{\sigma_2} ((x_2 - \mu_2)^2 - \sigma_2^2) \\ f_{12}(x_1, x_2) &= \frac{\beta_{12} (-\rho \sigma_2^2 ((\rho^2 - 1) \sigma_1^2 + (x_1 - \mu_1)^2) + (\rho^2 + 1) \sigma_1 \sigma_2 (x_1 - \mu_1)(x_2 - \mu_2) + \rho \sigma_1^2 (-(x_2 - \mu_2)^2))}{(\rho^2 + 1) \sigma_1 \sigma_2}. \end{aligned}$$

Computational details are contained in the appendices and these results are special cases of those in Li and Rabitz [2014]. Observe that HDMR projections contain elements not observed in f and that these additional elements are functions on X that depend upon the parameters of μ . For example, **$f_1(x_1)$ contains a quadratic term in x_1 , whereas $f(x)$ does not**. The sensitivity indices of f exhibit complex dependence on the model coefficients and distribution parameters,

$$\begin{aligned} \mathbb{S}_1^a &= \frac{\sigma_1^2 \left((\beta_1 + \beta_{12} \mu_2)^2 + \frac{2\beta_{12}^2 \rho^2 \sigma_2^2}{(\rho^2 + 1)^2} \right)}{2\rho\sigma_1\sigma_2(\beta_1 + \beta_{12}\mu_2)(\beta_2 + \beta_{12}\mu_1) + \sigma_1^2(\beta_1 + \beta_{12}\mu_2)^2 + \sigma_2^2((\beta_2 + \beta_{12}\mu_1)^2 + \beta_{12}^2(\rho^2 + 1)\sigma_1^2)} \\ \mathbb{S}_1^b &= \frac{\rho\sigma_1\sigma_2 \left((\rho^2 + 1)^2 (\beta_1 + \beta_{12}\mu_2)(\beta_2 + \beta_{12}\mu_1) + 2\beta_{12}^2 \rho^3 \sigma_1 \sigma_2 \right)}{(\rho^2 + 1)^2 (2\rho\sigma_1\sigma_2(\beta_1 + \beta_{12}\mu_2)(\beta_2 + \beta_{12}\mu_1) + \sigma_1^2(\beta_1 + \beta_{12}\mu_2)^2 + \sigma_2^2((\beta_2 + \beta_{12}\mu_1)^2 + \beta_{12}^2(\rho^2 + 1)\sigma_1^2))} \\ \mathbb{S}_{12}^a &= \frac{\beta_{12}^2 (\rho^2 - 1)^2 \sigma_1^2 \sigma_2^2}{(\rho^2 + 1) (2\rho\sigma_1\sigma_2(\beta_1 + \beta_{12}\mu_2)(\beta_2 + \beta_{12}\mu_1) + \sigma_1^2(\beta_1 + \beta_{12}\mu_2)^2 + \sigma_2^2((\beta_2 + \beta_{12}\mu_1)^2 + \beta_{12}^2(\rho^2 + 1)\sigma_1^2))} \\ \mathbb{S}_{12}^b &= 0, \end{aligned}$$

where

$$\mathbb{S}_i = \mathbb{S}_i^a + \mathbb{S}_i^b, \quad i \in \{1, 2, 12\}$$

and satisfy for general parameters

$$\mathbb{S}_1 + \mathbb{S}_2 + \mathbb{S}_{12} = 1.$$

Note that when $\rho = 0$, then $\mathbb{S}_1^b = \mathbb{S}_2^b = \mathbb{S}_{12}^b = 0$. **All non-trivial projections depend upon ρ and β .** In other words, the projections are functions of the measure μ and of the model f . Note that $\mathbb{S}_{12}^b = 0$ for any ρ due to the hierarchical-orthogonality of f_{12} , e.g., for every ρ we have $\langle f_{12}, f_1 \rangle = \langle f_{12}, f_2 \rangle = 0$ but $\langle f_1, f_2 \rangle = 0$ only for $\rho = 0$.

Consider $\rho \rightarrow 1$. We know from the direct form of $f(\beta, x)$ that in the limit we have $x_1 = x_2$ and $f(\beta, x) = \beta_0 + (\beta_1 + \beta_2)x + \beta_{12}x^2$. That is, f degenerates from a two-dimensional function into a one-dimensional function as the coherence indicated by ρ achieves unity. HDMR uniquely captures this behavior in a variance-preserving manner for general distributions. We illustrate this property in Figure 5 with plots of the sensitivity indices as functions of ρ for fixed μ , σ and β . Colored regions indicate increased variance (green) or reduced variance (red) relative to $\rho = 0$. For example, Figure 5f illustrates that the HDMR component function subspace in $X_1 \times X_2$ experiences annihilation for $|\rho| \rightarrow 1$.

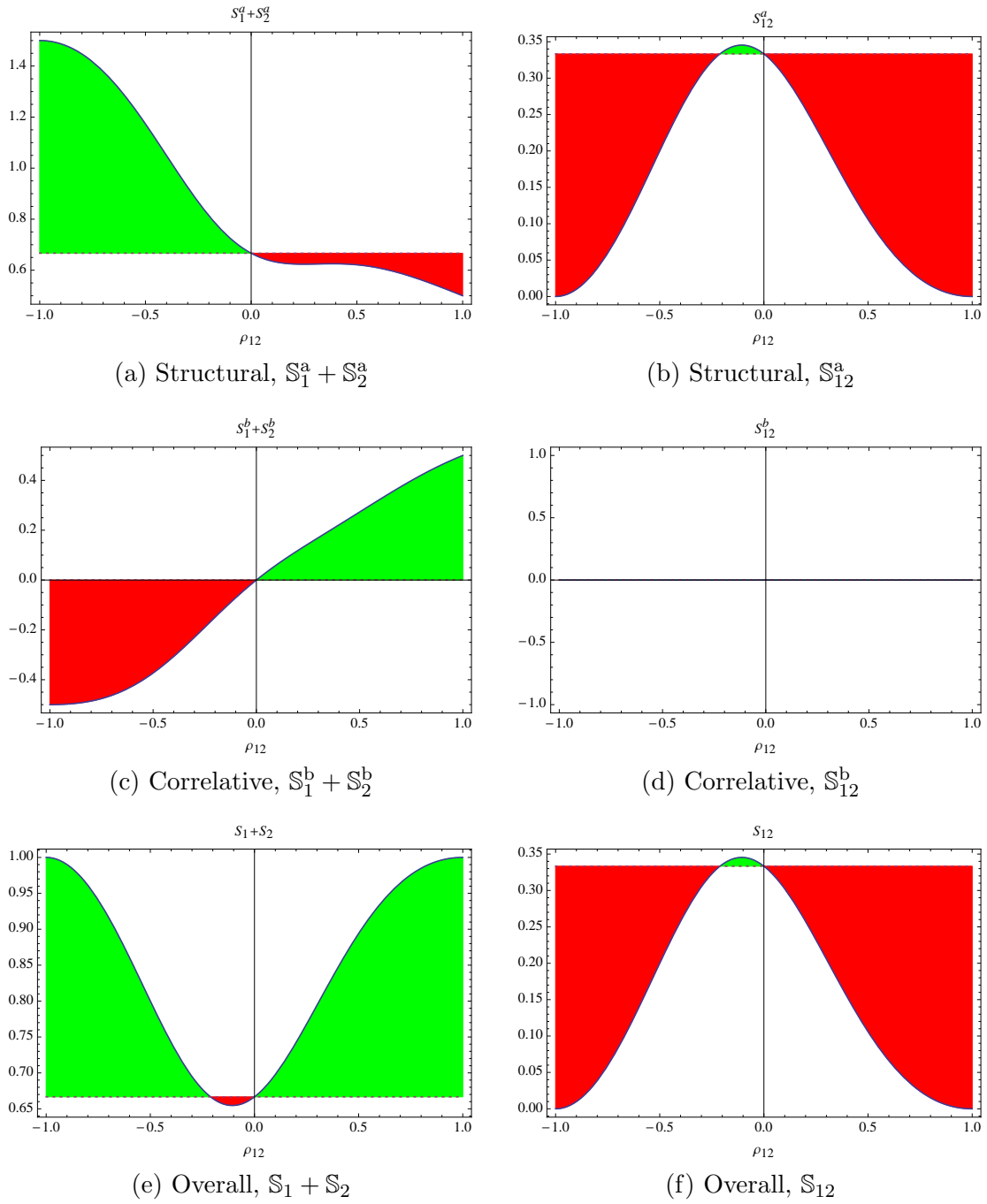


Figure 5: sensitivity indices for $\beta = \mathbf{1}$, $\mu = \mathbf{0}$ and $\sigma = \mathbf{1}$ as a function of ρ , colored to reflect the correlative contributions (positive and negative)

In the next section we make a study of (2) using other interpretative diagnostics in machine learning and compare to the results of this section.

4 Interpretative diagnostics

Interpretative diagnostics provide explanation for prediction [Guyon and Elisseeff, 2003]. Many common interpretative diagnostics are dependent upon the choice of F and are said to be class-dependent. For example, variable depth in decision nodes of ensembles of decision trees and node weight pruning in neural networks are commonly employed for supervised machine learning settings to attain measures of variable importance. Other interpretative diagnostics are defined in terms of an objective function J . For suitable J finite differences or derivative-based sensitivity analysis are conducted to assess the importance of various subsets of variables. We use the risk function R as the objective function J . We compare variable importance and dependence measures using \mathbf{I}^u and \mathbf{P}^u defined by partial dependence [Friedman, 2001], derivative-based global sensitivity indices [Sobol' and Kucherenko, 2009], and HDMR for the model (2). We illustrate that HDMR preserves explained variance independent of correlation in μ , whereas partial dependence is valid for modest correlation ($\rho < 0.3$).

4.1 Partial dependence

The partial dependence of $f(x)$ on x_u can be defined a couple ways [Friedman, 2001]. One is given by

$$\mathbf{P}_{\text{PD}}^u f(x) \equiv \mathbf{M}^u f(x) = \int_{X_{-u}} f(x) d\mu_{-u}(x_{-u}) = f_u^{\text{PD}}(x_u), \quad (3)$$

which is useful whenever the dependence between x_u and x_{-u} is not too strong. Another formulation of partial dependence is given by

$$\mathbf{P}_{\text{PD}}^u f(x) \equiv \mathbf{N}^u f(x) = \int_{X_{-u}} f(x) d\mu_{-u|u}(x_{-u}) = f_u^{\text{PD}}(x_u), \quad (4)$$

which considers the effect of dependencies. Here, the function is averaged with respect to the conditional distribution. If $\tilde{f}(x) = f(x) - f_0$ and the inputs are independent, then partial dependence is related to HDMR, where $\mathbf{P}_{\text{PD}}^i \tilde{f}(x) = \mathbf{P}_{\text{HDMR}}^i \tilde{f}(x) = \tilde{f}_i^{\text{HDMR}}(x_i)$ for $i \in \mathbb{N}_n$. Because of this relationship, we define the importance functional for partial dependence in a manner similar to HDMR,

$$\mathbf{I}_{\text{PD}}^i f(x) \equiv (S_i^{a\text{PD}}, S_i^{b\text{PD}}, S_i^{\text{PD}}).$$

4.2 Derivative-based global sensitivity measures

Sobol' and Kucherenko [2009] introduced derivative-based global sensitivity measures. Weighted derivative-based global sensitivity measures (DGSM) are defined as

$$\mathbf{I}_{\text{DGSM}}^u f(x) \equiv \int_X (D^{\alpha_u} f(x))^2 w_u(x_u) d\mu(x) = S_u^{\text{DGSM}},$$

where

$$D^{\alpha_u} f(x) = \frac{\partial^{|\alpha|} f(x)}{\partial x_1^{\alpha_{u1}} \dots \partial x_n^{\alpha_{un}}}$$

and $w_u(x_u)$ is a weight function. Putting $\mathbf{D}^\alpha \mathbf{f} = (D^{\alpha_u} f(x) : u)$, a normalized DGSM is given as

$$\mathbf{I}_{\text{DGSM}}^u f(x) \equiv \frac{\int_X (D^{\alpha_u} f(x))^2 w_u(x_u) d\mu(x)}{\|\mathbf{D}^\alpha \mathbf{f}\|_{2;F}^2} = S_u^{\text{DGSM}},$$

where

$$\|\mathbf{f}\|_{2;F} = \left(\sum_{f \in \mathbf{f}} \|f\|_{L^2(\Omega, \mathcal{F}, \mu)}^2 \right)^{1/2}.$$

We take $w_u(x_u) = 1$.

4.3 Illustration

We illustrate these interpretative diagnostics for equation (2),

$$f(\beta, x) = \beta_0 + \beta_1 x_1 + \beta_2 x_2 + \beta_{12} x_1 x_2.$$

We take $\beta = \mathbf{1}$, $\mu = \mathbf{1}$, and $\sigma = \mathbf{1}$, and examine variable importance as a function of correlation, ρ . For DGSM, we also consider $\sigma_f^2(\beta) = \beta_2^2 + 2\beta_2\beta_3\rho + \beta_3^2 + \beta_{12}^2(\rho^2 + 1)$. Whenever $\rho \in \{-1, 1\}$ such that $x_1 = x_2$ the function is one-dimensional and all variable importance resides in the univariate importance measures. The component functions are analytically given by

$$\begin{aligned} \tilde{f}_1^{\text{HDMR}}(x_1) &= x_1 + \frac{\rho}{\rho^2 + 1}(x_1^2 - 1) \\ \tilde{f}_1^{\text{PD (marg.)}}(x_1) &= x_1 \\ \tilde{f}_1^{\text{PD (cond.)}}(x_1) &= x_1 + \rho(x_1^2 + x_1 - 1). \end{aligned}$$

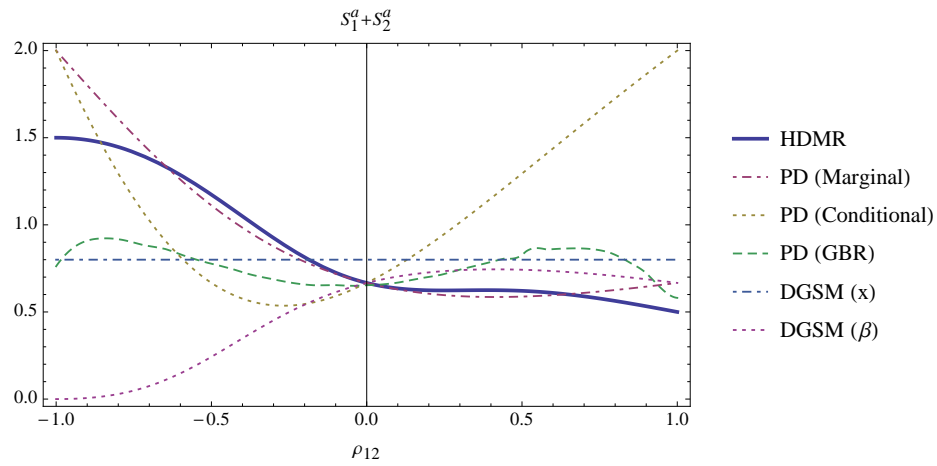
Notice that the HDMR component function has non-linear dependence on ρ , whereas PD exhibits linear dependence. Variable importance results are exhibited in Table 3 and Figure 6 (note that the minimum and curvature for the 'U'-shaped behavior changes in β and

for $\beta = \mathbf{1}$ in Figure 6c it is not symmetric), and variable dependence results are exhibited in Figure 7. For HDMR and partial dependence, we breakdown the importance measure into structural and correlative terms. We compute importance measures for $\rho \in \{-1, 0, 1\}$. All importance measures, with the exception of $\mathbf{I}_{\text{DGSM}}f(x)$, depend upon ρ . When $\rho = 0$, all coincide except $\mathbf{I}_{\text{DGSM}}f(x)$. Only HDMR preserves variance, $S(-1) = S(1) = 1$.

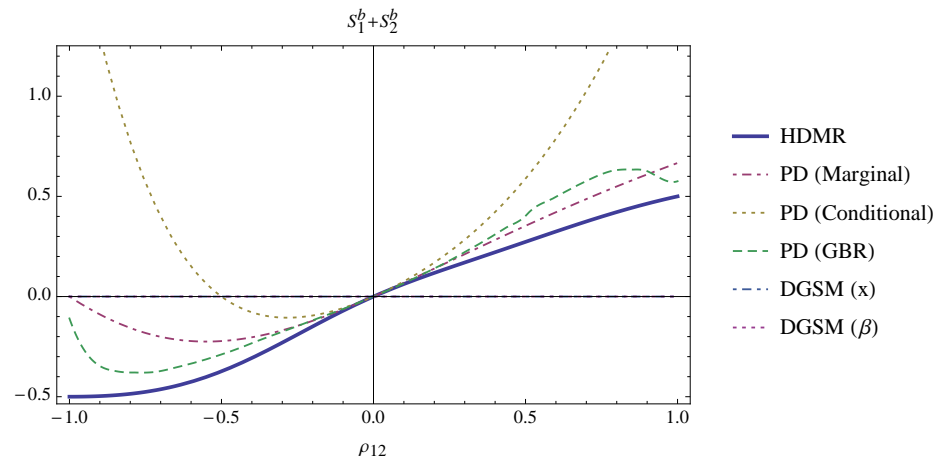
The variance decomposition property of HDMR, i.e. $S(-1) = S(1) = 1$, means that the HDMR expansion correctly captures the contributions of subsets of variables to the variance in the output. **Observe that partial dependence given by (3) is accurate when correlation is roughly less than 0.3.** As the strength of dependence grows, the univariate partial dependency interpretative diagnostics of (3) become increasingly distorted. The diagnostic given by (4) exhibits far less variance stability in one-dimensional subspaces than that given by (3). PD is also estimated using a gradient boosting machine (PD (GBR), where GBR-estimated PD is estimated thirty times on a grid for ρ , each GBR having 500 estimators of max depth of four and 10^3 independent random samples. PD (GBR) sensitivity indices are computed from the GBR-estimated PD's using quadrature. GBR estimation of PD (3) is significantly biased as correlation increases. DGSM gives different importance of $f(x)$ than HDMR and partial dependence, even for $\rho = 0$, although it coincides for $\sigma_f^2(\beta)$.

Figure 7 reveals the profile of $\tilde{f}_1(x_1)$ in ρ for HDMR and partial dependence (marginal, conditional, and GBR-estimated). PD (3) does not change in ρ , whereas PD (4) does. PD (GBR) significantly deviates from both HDMR and PD (3). When $\rho = 0$, the four coincide.

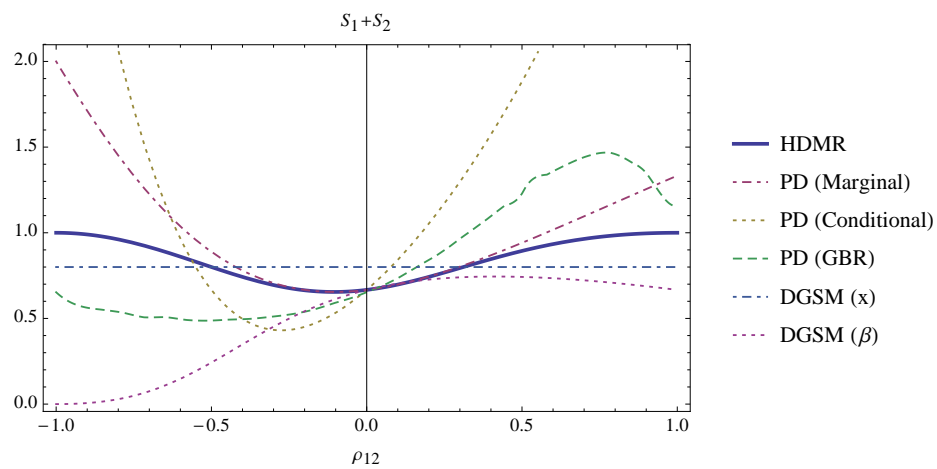
These results illustrate that **PD-based interpretative diagnostics experience information leakage whenever $\rho > 0$.** In a similar manner, GBR-estimated PD exhibits information leakage. It is interesting that GBR-estimated PD diverges from both analytic PD-measures. This may be attributed to biases in the underlying algorithmic implementation, as tree-based ensemble methods such as random forest are known to exhibit biases in variable importance [Strobl et al., 2007].



(a) Structural, $S_1^a + S_2^a$

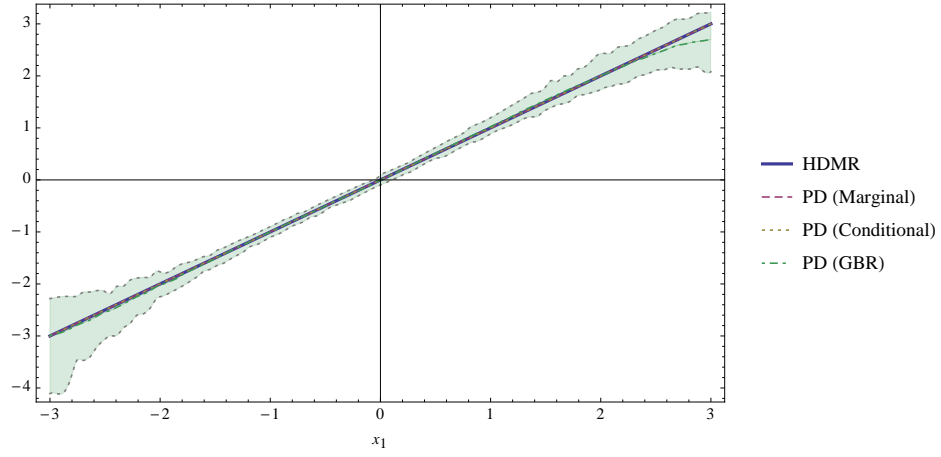


(b) Correlative, $S_1^b + S_2^b$

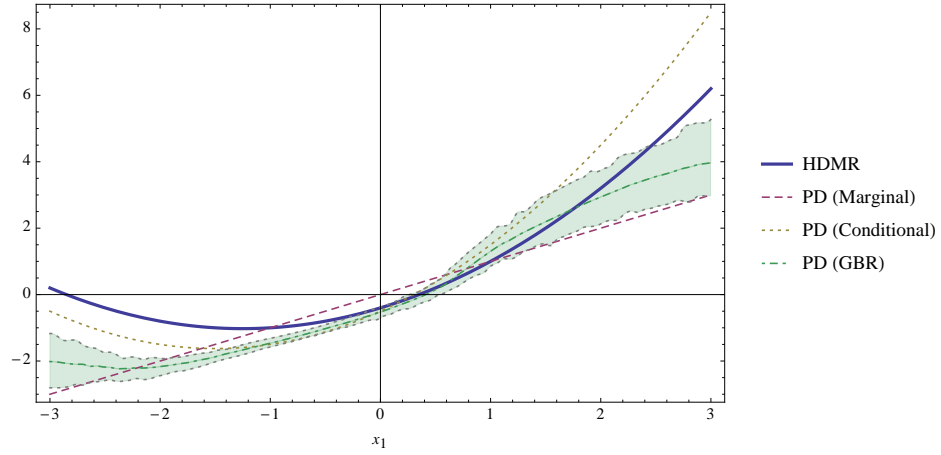


(c) Overall, $S_1 + S_2$

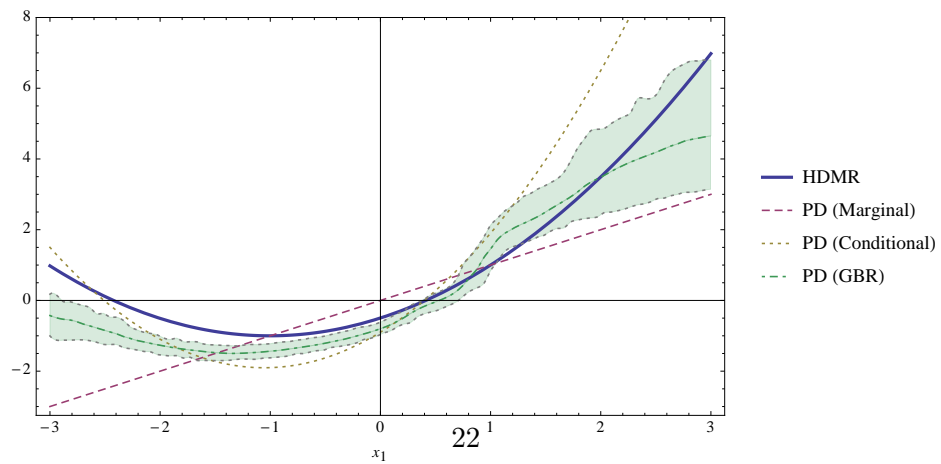
Figure 6: Univariate variable importance by HDMR, PD, and DGSM for $\beta = 1$, $\mu = \mathbf{0}$ and $\sigma = \mathbf{1}$ as a function of ρ .



(a) $\rho = 0$



(b) $\rho = \frac{1}{2}$



(c) $\rho = \frac{9}{10}$

Figure 7: Variable dependence $\tilde{f}_1(x_1)$ for $\rho \in \{0, \frac{1}{2}, \frac{9}{10}\}$ for HDMR, PD (Marginal), PD (Conditional), and PD (GBR) ($(\alpha, 1 - \alpha)$ percentile, $\alpha = 0.025$)

Table 3: Variable importance measures in ρ for $\beta = \mathbf{1}$, $\mu = \mathbf{1}$, and $\sigma = \mathbf{1}$.

Variable Importance	$S^a(\rho)$	$S^b(\rho)$	$S(\rho)$	$S(-1)$	$S(0)$	$S(1)$
$\mathbf{I}_{\text{HDMR}}^1 + \mathbf{I}_{\text{HDMR}}^2$	$\frac{2(\rho^4 + 4\rho^2 + 1)}{(\rho^2 + 1)^2(\rho(\rho + 2) + 3)}$	$\frac{2\rho(2\rho^3 + (\rho^2 + 1)^2)}{(\rho^2 + 1)^2(\rho(\rho + 2) + 3)}$	$\frac{\rho - 1}{\rho^2 + 1} + \frac{\rho + 5}{\rho(\rho + 2) + 3}$	1	2/3	1
$\mathbf{I}_{\text{PD}}^1 + \mathbf{I}_{\text{PD}}^2$ (marg.)	$\frac{2(\rho^2 + 1)}{\rho(\rho + 2) + 3}$	$\frac{2(\rho(\rho + 1))}{\rho^2 + 2\rho + 3}$	$\frac{2(2\rho^2 + \rho + 1)}{\rho(\rho + 2) + 3}$	2	2/3	4/3
$\mathbf{I}_{\text{PD}}^1 + \mathbf{I}_{\text{PD}}^2$ (cond.)	$\frac{6\rho^2 + 4\rho + 2}{\rho^2 + 2\rho + 3}$	$\frac{2(\rho(2\rho^3 + \rho^2 + 2\rho + 1))}{\rho^2 + 2\rho + 3}$	$\frac{2(\rho(\rho(2\rho^2 + \rho + 5) + 3) + 1)}{\rho(\rho + 2) + 3}$	4	2/3	4
$\mathbf{I}_{\text{PD}}^1 + \mathbf{I}_{\text{PD}}^2$ (GBR)	-	-	-	0.65	0.65	1.14
$\mathbf{I}_{\text{DGSM}}^1 + \mathbf{I}_{\text{DGSM}}^2$	4/5	0	4/5	4/5	4/5	4/5
$\mathbf{I}_{\text{DGSM}}^1 + \mathbf{I}_{\text{DGSM}}^2$	$\frac{2(\rho + 1)^2}{\rho(\rho^3 + 4\rho + 4) + 3}$	0	$\frac{2(\rho + 1)^2}{\rho(\rho^3 + 4\rho + 4) + 3}$	0	2/3	2/3

5 Glass boxes from black boxes

General-purpose black box learning algorithms in machine learning, such as kernel machines or decision tree models, exhibit favorable predictive performances and configuration or tuning costs. Suppose the availability of a black box representation $f \in F$. We demonstrate how HDMR assesses variable importance and dependence of kernel machines or ensembles of decision trees. In this manner, HDMR is said to be a wrapper method [Guyon and Elisseeff, 2003]. We give HDMR constructions for kernel machines and ensembles of decision trees and provide illustrations for polynomial kernel machines and ensembles of gradient boosting machines.

5.1 Kernel machines

HDMR provide interpretative diagnostics for the output of a kernel machine through a decomposition of the inner product of its RKHS. This is similar to the approach used in smoothing spline ANOVA RKHS but such is based on orthogonal projections [Wahba, 1990, Wahba et al., 1995]. We outline the approach below and discuss polynomial kernels.

Assume we have a kernel

$$K(x, x') = \langle \phi(x), \phi(x') \rangle_{\ell^2},$$

where $\phi : X \mapsto \ell^2(\alpha)$ is a feature map with index set α of size $b \in \mathbb{N}$ and $\phi(x) = (\phi_\alpha(x) : \alpha \in \alpha)$ is a feature vector. We assume these feature vectors are represented by the Hadamard (entrywise) product of constants and basis elements, $\phi(x) = \beta \odot \mathbf{B}(x)$, where $\mathbf{B}(x) = (\mathbf{B}_\alpha(x) : \alpha \in \alpha)$ are bases and $\beta \in \mathbb{R}^b$ are coefficients (note that $\mathbf{B}(x)$ is known as a Mercer map). The HDMR of the kernel is attained by decomposing the feature vector as

$$\phi(x) = \sum_{\alpha \in \alpha} \nu_\alpha \psi_\alpha(x) = \sum_{\alpha \in \alpha} \nu_\alpha (\eta_\alpha \odot \mathbf{B}(x)), \quad (5)$$

where $\{\psi_\alpha(x) \equiv \boldsymbol{\eta}_\alpha \odot \mathbf{B}(x)\}$ are component feature vectors and $\{\boldsymbol{\eta}_\alpha = (\eta_{\alpha\alpha'} : \alpha' \in \boldsymbol{\alpha})\}$ are coefficient vectors attained from μ . These coefficients reflect the hierarchical-orthogonality of the feature vectors and their generation is detailed in the appendices. Putting $\mathbf{A} \equiv (\boldsymbol{\eta}_\alpha) \in \mathbb{R}^{b \times b}$, we have

$$\boldsymbol{\beta} = \mathbf{A} \boldsymbol{\nu} \quad (6)$$

where $\boldsymbol{\nu} = (\nu_\alpha : \alpha \in \boldsymbol{\alpha}) \in \mathbb{R}^b$. Given i) $\boldsymbol{\beta}$ from the kernel and ii) \mathbf{A} from the measure μ , this system is solved for $\boldsymbol{\nu}$,

$$\boldsymbol{\nu} = \mathbf{A}^{-1} \boldsymbol{\beta}.$$

Using $\{\nu_\alpha \psi_\alpha(x)\}$, we form the **HDMR of K** by putting

$$\phi(x) \equiv \sum_{u \subseteq \mathbb{N}_n} \Psi_u(x),$$

where the collection $\{\Psi_u(x)\}$ is formed as

$$\left\{ \Psi_u(x) : \forall u \subseteq \mathbb{N}_n, \boldsymbol{\alpha}_u \subset \boldsymbol{\alpha}, \Psi_u(x) \equiv \sum_{\alpha \in \boldsymbol{\alpha}_u} \nu_\alpha \psi_\alpha(x) \right\}. \quad (7)$$

If a subset of component feature vectors is sought, $\{\Psi_u(x) : |u| \leq T < d\}$, then we have $\mathbf{A} \in \mathbb{R}^{a \times b}$, an underdetermined system $a < b$, and a least-norm solution can be efficiently attained using QR decomposition. Given a finite dataset \mathbf{D} and a kernel K , a kernel machine attains a set coefficients $\{\xi_{x'}\}$ such that

$$\begin{aligned} f(x) &= \sum_{x' \in \mathbf{D}} \xi_{x'} K(x, x') \\ &= \sum_{x' \in \mathbf{D}} \xi_{x'} \langle \phi(x), \phi(x') \rangle_{\ell^2} \\ &= \left\langle \sum_{u \subseteq \mathbb{N}_n} \Psi_u(x), \sum_{x' \in \mathbf{D}} \xi_{x'} \phi(x') \right\rangle_{\ell^2} \\ &= \sum_{u \subseteq \mathbb{N}_n} \langle \Psi_u(x), f \rangle_{\ell^2} \\ &= \sum_{u \subseteq \mathbb{N}_n} f_u^{\text{HDMR}}(x_u). \end{aligned}$$

Polynomial kernels

The (real-valued) polynomial kernel is given by

$$K_{\text{poly}}(x, x'; c, d, \gamma) = (\gamma x \cdot x' + c)^d, \quad (8)$$

where $c, \gamma \geq 0$, $d \in \mathbb{N}$, and $x, x' \in \mathbb{R}^n$. Defining $\boldsymbol{\alpha}(n, d) = \{\alpha \in \mathbb{N}_0^{n+1}, |\alpha| = d\}$,

$$\mathbf{B}(x; n, d) = (x^{\alpha_1 \cdots \alpha_n} : \alpha \in \boldsymbol{\alpha}(n, d))$$

and

$$\begin{aligned} \boldsymbol{\beta}(n, d) &= (\beta_\alpha : \alpha \in \boldsymbol{\alpha}(n, d)), \\ \beta_\alpha &= \left(\binom{d}{\alpha} c^{\alpha_0} \gamma^{d-\alpha_0} \right)^{1/2}, \end{aligned}$$

we have (suppressing notation in n and d)

$$\boldsymbol{\phi}(x) = \boldsymbol{\beta} \odot \mathbf{B}(x).$$

Together,

$$\begin{aligned} K_{\text{poly}}(x, x'; c, d, \gamma) &= \langle \boldsymbol{\phi}(x), \boldsymbol{\phi}(x') \rangle_{\ell^2} \\ &= \sum_{\alpha \in \boldsymbol{\alpha}} \beta_\alpha^2 x^{\alpha_1 \cdots \alpha_n} x'^{\alpha_1 \cdots \alpha_n}. \end{aligned}$$

Defining $\mathbf{C}(x; n, d) = (e^{2\pi i \langle \alpha_1 \cdots \alpha_n, x \rangle} : \alpha \in \boldsymbol{\alpha}(n, d))$ and $\boldsymbol{\phi}(x) = \boldsymbol{\beta} \odot \mathbf{C}(x)$, we write a complex-valued polynomial kernel,

$$\begin{aligned} K_{\text{poly}}(x, x'; c, d, \gamma) &= \langle \boldsymbol{\phi}(x), \boldsymbol{\phi}(x') \rangle_{\ell^2} \\ &= (\gamma e^{2\pi i x} \cdot e^{2\pi i x'} + c)^d \\ &= \sum_{\alpha \in \boldsymbol{\alpha}} \beta_\alpha^2 e^{2\pi i \langle \alpha_1 \cdots \alpha_n, x \rangle} e^{2\pi i \langle \alpha_1 \cdots \alpha_n, x' \rangle} \\ &= \sum_{\alpha \in \boldsymbol{\alpha}} \beta_\alpha^2 e^{2\pi i \langle \alpha_1 \cdots \alpha_n, x+x' \rangle}. \end{aligned}$$

Illustration: analytic function

We consider the mathematical function (2). In Figure 8, we compare $f_1(x_1)$ as computed by kernel machines— $f_1^{\text{HDMMR}}(x_1)$, attained from the empirical HDMMR (16) (“empirical-polynomial HDMMR”) and $f_1^{\text{ANOVA}}(x_1)$, attained from the ANOVA representation of the polynomial kernel (8) (“ANOVA-polynomial kernel”). The ANOVA-kernel of the polynomial kernel is defined as $K_{\text{ANOVA}}(x, x') = \prod_{i \in \mathbb{N}_n} (1 + k_i(x_i, x'_i))$ [Durrande et al., 2013], where $\{k_i(x_i, x'_i)\}$ are univariate zero-mean polynomial kernels. Both kernel machines use the same empirical measure of 10^3 data elements with $\rho = \frac{1}{2}$ and are compared to the exact HDMMR. As seen in Figure 8, **the ANOVA-polynomial kernel does not use the correlative information of the input data**, whereas the empirical-polynomial HDMMR better approximates the exact underlying HDMMR.

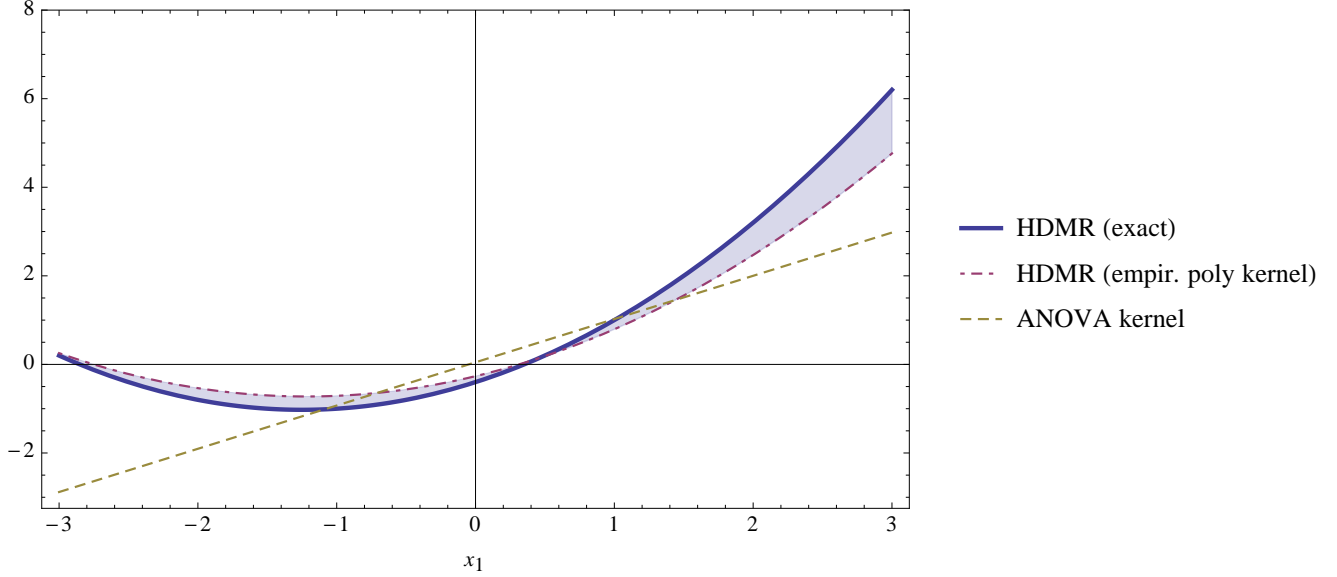


Figure 8: Plot of $f_1(x_1)$ for $\rho = \frac{1}{2}$; HDMR (exact) compared to ANOVA-polynomial kernel and empirical-polynomial HDMR

5.2 Decision trees

A decision tree is a function that uses a partition of $X = \cup_{R_i \in R} R_i$, $R = \{R_i\}_i$, such that

$$g(x) = \sum_{R_i \in R} c_i \mathbb{1}_{R_i}(x).$$

The partition R_u is defined using a subset of variables x_u such that a tree is written as

$$g_u(x_u) \equiv \sum_{R_i \in R_u} c_i \mathbb{1}_{R_i}(x_u).$$

A collection of tree ensembles, indexed by \mathcal{I} , is denoted by

$$F_{\mathcal{I}} \equiv \{f^i(x)\}_{i \in \mathcal{I}}, \quad (9)$$

where $f^i(x)$ is a sum of trees across the subspaces $\mathcal{P}_i \subseteq \mathcal{P}(\mathbb{N}_n)$

$$f^i(x) \equiv \sum_{u \in \mathcal{P}_i} g_u^i(x_u) = \sum_{u \in \mathcal{P}_i} \sum_j g_{uj}^i(x_u)$$

and has depth $d \in \mathbb{N}$ [Breiman, 2001]. A key property of trained decision tree models is that tree subspaces are highly sparse, $|\mathcal{P}_i| \ll |\mathcal{P}(\mathbb{N}_n)|$ for $i \in \mathbb{N}_n$. A linear combination of

tree ensembles is defined as

$$f(x) \equiv \sum_{i \in \mathcal{I}} \beta_i f^i(x). \quad (10)$$

Forming $\mathbf{F}_{\mathcal{I}} \equiv (f^i : i \in \mathcal{I}) = (g_u^i : i \in \mathcal{I}, u \in \mathcal{P}_i)$ we take

$$\boldsymbol{\beta}(\lambda) \equiv (\beta_{ui}(\lambda) : i \in \mathcal{I}, u \in \mathcal{P}_i) = (\mathbf{F}_{\mathcal{I}} \otimes \mathbf{F}_{\mathcal{I}} + \lambda I)^{-1}(\mathbf{F}_{\mathcal{I}} \otimes f).$$

We index the tree ensemble feature vectors on $\boldsymbol{\alpha}$ as

$$\boldsymbol{\alpha} \equiv (\boldsymbol{\alpha}_0) \parallel ((i, u) \in \mathcal{I} \times \wp(\mathbb{N}_n) : i \in \mathcal{I}, u \in \mathcal{P}_i)$$

where

$$\boldsymbol{\alpha}_0 = (\{\}, \{\})$$

and define

$$\begin{aligned} \boldsymbol{\alpha}_{\bullet u} &\equiv \{(i, w) \in \boldsymbol{\alpha} : i \in \mathcal{I}, w = u\} \\ \boldsymbol{\alpha}_{i \bullet} &\equiv \{(j, u) \in \boldsymbol{\alpha} : u \in \mathcal{P}_j, j = i\}. \end{aligned}$$

The tree ensemble feature vectors are given by

$$\begin{aligned} \phi^i(x) &\equiv \boldsymbol{\beta}^i(\lambda) \odot \mathbf{B}^i(x) \\ \mathbf{B}^i(x) &\equiv (g_u^i(x_u) 1_{\boldsymbol{\alpha}_{i \bullet}}(j, u) : (j, u) \in \boldsymbol{\alpha}) \\ \boldsymbol{\beta}^i(\lambda) &\equiv (\beta_i(\lambda) 1_{\boldsymbol{\alpha}_{i \bullet}}(j, u) : (j, u) \in \boldsymbol{\alpha}). \end{aligned}$$

This is written as

$$\phi(x) = \sum_{i \in \mathcal{I}} (\boldsymbol{\beta}^i(\lambda) \odot \mathbf{B}^i(x)) = \boldsymbol{\beta}(\lambda) \odot \mathbf{B}(x),$$

where

$$\mathbf{B}(x) = \sum_{i \in \mathcal{I}} \mathbf{B}^i(x)$$

and

$$\boldsymbol{\beta}(\lambda) = \sum_{i \in \mathcal{I}} \boldsymbol{\beta}^i(\lambda). \quad (11)$$

Note that $\boldsymbol{\beta}_0 = 0$. As before, we have the coefficients attained from μ as $\boldsymbol{\eta}_{\alpha}$ and in organized form,

$$\mathbf{A} \equiv (\boldsymbol{\eta}_{\alpha}). \quad (12)$$

Then, weights $\boldsymbol{\nu} = (\nu_{\alpha} : \alpha \in \boldsymbol{\alpha})$ are attained that satisfy

$$\boldsymbol{\beta}(\lambda) = \mathbf{A} \boldsymbol{\nu} \quad (13)$$

as

$$\boldsymbol{\nu} = \mathbf{A}^{-1}\boldsymbol{\beta}(\lambda). \quad (14)$$

Noting

$$\phi(x) = \sum_{\alpha \in \boldsymbol{\alpha}} \nu_{\alpha} \psi_{\alpha}(x) = \sum_{\alpha \in \boldsymbol{\alpha}} \nu_{\alpha} (\boldsymbol{\eta}_{\alpha} \odot \mathbf{B}(x)), \quad (15)$$

we form the **HDMMR of $F_{\mathcal{I}}$** as

$$\left\{ \Psi_u(x) : \forall u \subseteq \mathbb{N}_n, \boldsymbol{\alpha}_u \subset \boldsymbol{\alpha}, \Psi_u(x) \equiv \sum_{\alpha \in \boldsymbol{\alpha}_u} \nu_{\alpha} \psi_{\alpha}(x) \right\}. \quad (16)$$

We summarize the computations:

- (i) Equation (9): forming $F_{\mathcal{I}}$ from the collection of GBR models $\{f^i(x)\}_{i \in \mathcal{I}}$, indexed on \mathcal{I}
- (ii) Equations (10) and (11): linearly combining the elements of $F_{\mathcal{I}}$ as $f(x)$ using the coefficients $\boldsymbol{\beta}(\lambda) \equiv (\beta_{ui}(\lambda) : i \in \mathcal{I}, u \in \mathcal{P}_i) \in \mathbb{R}^b$, attained from regularized least-squares using with grid-searched λ estimated using K -fold cross-validation
- (iii) Equation (12): attaining $\boldsymbol{\eta}_{\alpha}$ from the measure μ using a collection of QR-decompositions, each identified to a component function subspace and each QR decomposition having linear cost in the dataset size $\mathcal{O}(N)$ and quadratic cost $\mathcal{O}(|\mathcal{P}(x_u) \cap \mathcal{P}_i|^2)$ (typically small in most HDMMR applications) and forming the square matrix $\mathbf{A} \in \mathbb{R}^{b \times b}$, where b is total size of the corresponding inner product space $|\cup_i \mathcal{P}_i|$
- (iv) Equations (13) and (14): forming the system $\boldsymbol{\beta} = \mathbf{A} \cdot \boldsymbol{\nu}$, computing the inverse of the square matrix \mathbf{A} , such as through using Gaussian elimination, and putting $\boldsymbol{\nu} \equiv \mathbf{A}^{-1}\boldsymbol{\beta}$
- (v) Equations (15) and (16): forming the HDMMR $\mathbf{F}_{\mathcal{I}}$.

Projections into the space of decision trees, which are systems of simple functions, produce noisy approximations to continuous functions. This can be addressed through spectral filtering of the component function subspaces, such as projection into smooth subspaces (Fourier). Another consideration is that if the GBR ensemble experience information leakage on the subspaces of F the interpretative diagnostics will be biased (as illustrated in the previous section for non-trivial correlation). The variance-preserving property of HDMMR, however, enables introspection of black box learning algorithms for independent and/or correlated variables, to the extent that the black box contains information on the projections of the system.

We compute the HDMMR of two efficient general-purpose black-box supervised machine learning algorithms—the random forest (RF) and the gradient boosting regressor (GBR)

machine—for a non-linear mathematical function (Ishigami) with analytic solution and a benchmark dataset (California housing). We demonstrate that RF experiences far more information leakage than GBR and that GBR well approximates HDMR.

Illustration 1: analytic test function

In this example we verify that the HDMR of $F_{\mathcal{I}}$ given by (16) well approximates the true HDMR for a test function. We consider the Ishigami function, a non-linear continuous function, which exists in closed-form and is sparse. It is defined as

$$f(x) = \sin x_1 + a \sin^2 x_2 + b x_3^4 \sin x_1$$

with independent uniformly distributed $x = (x_1, x_2, x_3) \in [-\pi, \pi]^3$. Its HDMR is analytic and shown below,

$$\begin{aligned} f_0^{\text{HDMR}} &= \frac{a}{2} \\ f_1^{\text{HDMR}}(x_1) &= \left(1 + \frac{b\pi^4}{5}\right) \sin x_1 \\ f_2^{\text{HDMR}}(x_2) &= -\frac{a}{2} \cos 2x_2 \\ f_3^{\text{HDMR}}(x_3) &= 0 \\ f_{12}^{\text{HDMR}}(x_1, x_2) &= 0 \\ f_{13}^{\text{HDMR}}(x_1, x_3) &= b\left(x_3^4 - \frac{\pi^4}{5}\right) \sin x_1 \\ f_{23}^{\text{HDMR}}(x_2, x_3) &= 0 \\ f_{123}^{\text{HDMR}}(x_1, x_2, x_3) &= 0. \end{aligned}$$

Its non-trivial sensitivity indices are

$$\begin{aligned} \mathbb{S}_1 &= \frac{36 (\pi^4 b + 5)^2}{5 (45 (a^2 + 4) + 20\pi^8 b^2 + 72\pi^4 b)} \\ \mathbb{S}_2 &= \frac{45a^2}{45 (a^2 + 4) + 20\pi^8 b^2 + 72\pi^4 b} \\ \mathbb{S}_{13} &= \frac{64\pi^8 b^2}{5 (45 (a^2 + 4) + 20\pi^8 b^2 + 72\pi^4 b)} \end{aligned}$$

We utilize an ensemble of GBR's indexed on

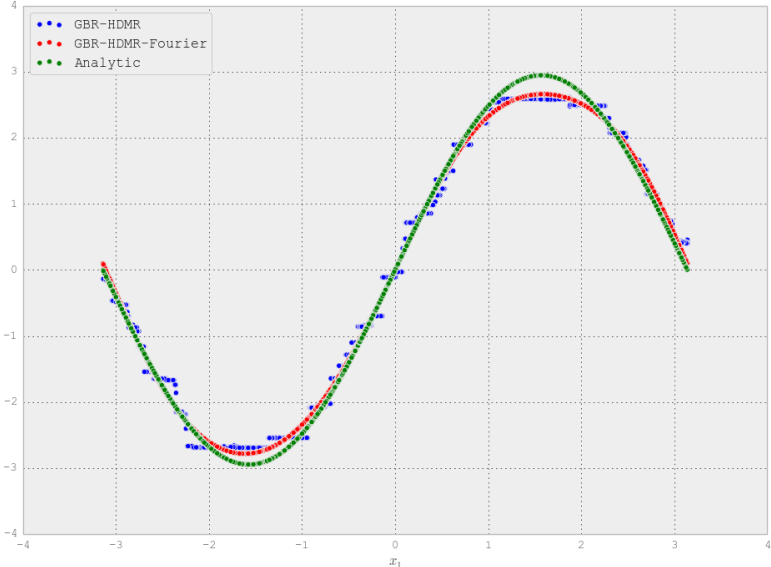
$$\begin{aligned} \mathcal{I}_i &= \{(\text{depth}_i, \text{subspaces})\} \\ &= \{(k, (1, 2, 3)) : k \in [i]\}. \end{aligned}$$

These are linearly combined using regularized least-squares with grid-searched λ . $J = 10^3$ trees are used in each ensemble and $N = 5 \times 10^3$ data points are sampled from $\text{Uniform}[-\pi, \pi]^3$.

In Figures 9 and 10 we estimate $f_1^{\text{HDMMR}}(x_1)$, $f_2^{\text{HDMMR}}(x_2)$, and $f_{13}^{\text{HDMMR}}(x_1, x_3)$ using GBR from $F_{\mathcal{I}_3}$. We also estimate these using RF (located in the appendices; Figures 18, 19, and 20). We project the one-dimensional component functions into the space of zero-mean band-limited Fourier series (degree four) to attain smooth low-frequency approximations. Sensitivity indices are shown below in Table 4. **The GBR-based decision tree approximations closely approximate the true HDMMR component functions, whereas RF performs poorly, experiencing significant information leakage in comparison to GBR.** GBR estimation of the two-dimensional component function $f_{13}^{\text{HDMMR}}(x_1, x_3)$ experiences some information leakage but its general qualitative behavior is satisfactorily reproduced as shown in Figure 10a. A tree-based measure of variable importance based on the fraction of samples variables contribute through trees is computed as ‘Tree’ and gives substantially different results than R by HDMMR: x_3 is the most important variable by fraction of samples but the least important by HDMMR. The defect in RF is appears to be insensitive to the number of trees, sample size, or tree depth.

Figure 9: One-dimensional component functions: GBR approximation, smooth Fourier projection, and analytic

(a) $f_1^{\text{HDMR}}(x_1)$



(b) $f_2^{\text{HDMR}}(x_2)$

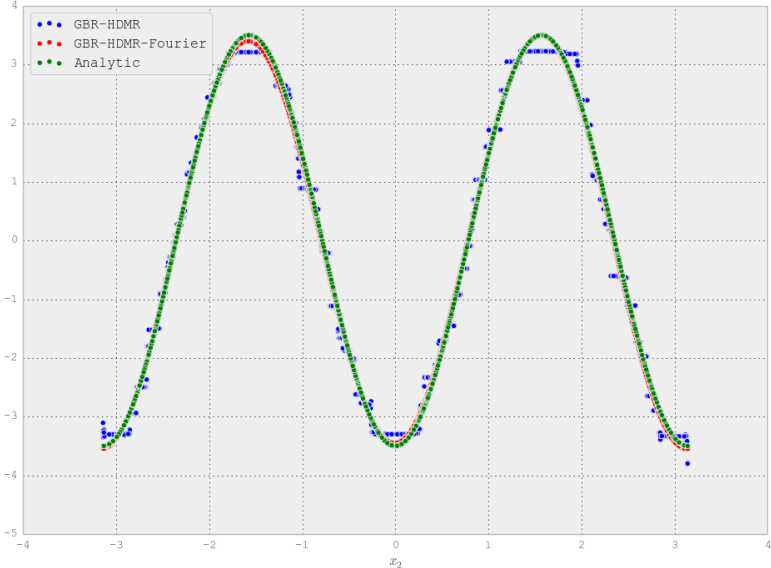
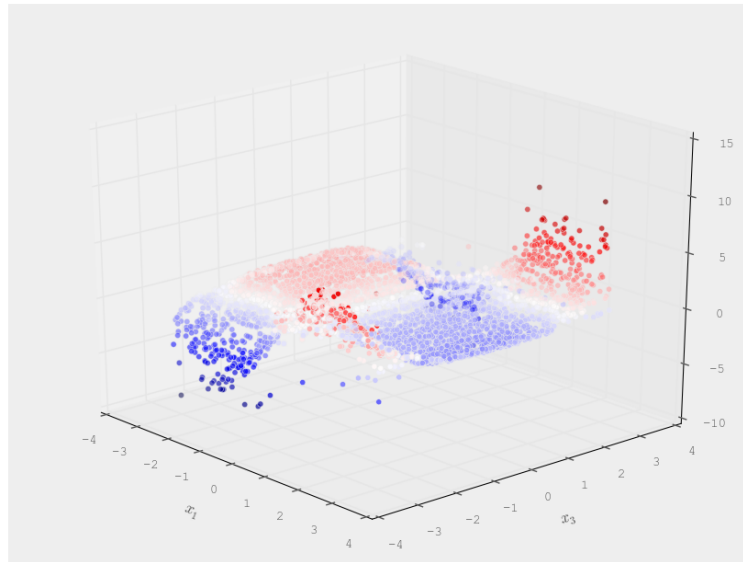


Figure 10: $f_{13}^{\text{HDMR}}(x_1, x_3)$ by GBR approximation

(a) Decision tree approximation



(b) Analytic

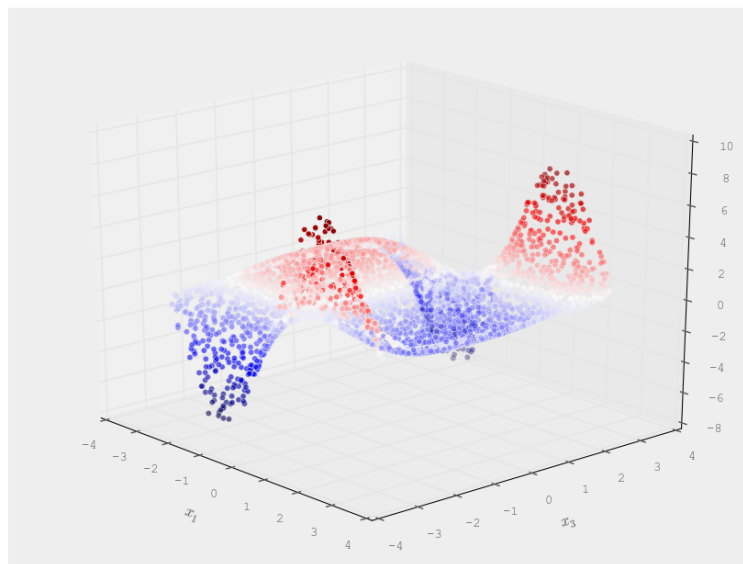


Table 4: Structural and correlative sensitivity analysis P_ϵ for the Ishigami function ($a = 7$, $b = 10^{-1}$) using gradient boosting regressor (GBR) machine and mean and standard deviation estimated from 50 random realizations for \mathcal{I}_1 , \mathcal{I}_2 , and \mathcal{I}_3

Subspace	Index	\mathbb{S}^a	\mathbb{S}^b	\mathbb{S}	T	R	Tree
(1.)	(Analytic)	0.31	0.00	0.31	0.56	0.45	
	\mathcal{I}_1	0.31 ± 0.00	0.00 ± 0.00	0.31 ± 0.00	0.31 ± 0.00	0.40 ± 0.00	0.23 ± 0.00
	\mathcal{I}_2	0.29 ± 0.00	0.01 ± 0.00	0.30 ± 0.00	0.49 ± 0.01	0.42 ± 0.00	0.33 ± 0.01
	\mathcal{I}_3	0.29 ± 0.00	0.01 ± 0.00	0.30 ± 0.00	0.51 ± 0.01	0.42 ± 0.00	0.32 ± 0.01
(2.)	(Analytic)	0.44	0.00	0.44	0.44	0.36	
	\mathcal{I}_1	0.46 ± 0.00	-0.00 ± 0.00	0.45 ± 0.00	0.45 ± 0.00	0.58 ± 0.00	0.57 ± 0.00
	\mathcal{I}_2	0.44 ± 0.00	0.00 ± 0.00	0.45 ± 0.00	0.45 ± 0.00	0.38 ± 0.00	0.25 ± 0.01
	\mathcal{I}_3	0.44 ± 0.00	0.00 ± 0.00	0.45 ± 0.00	0.46 ± 0.00	0.38 ± 0.00	0.28 ± 0.01
(3.)	(Analytic)	0.00	0.00	0.00	0.24	0.20	
	\mathcal{I}_1	0.01 ± 0.00	0.00 ± 0.00	0.02 ± 0.00	0.02 ± 0.00	0.02 ± 0.00	0.21 ± 0.00
	\mathcal{I}_2	0.03 ± 0.00	0.01 ± 0.00	0.04 ± 0.01	0.23 ± 0.00	0.20 ± 0.00	0.42 ± 0.01
	\mathcal{I}_3	0.03 ± 0.00	0.01 ± 0.00	0.04 ± 0.01	0.25 ± 0.00	0.20 ± 0.00	0.40 ± 0.01
(1,2)	(Analytic)	0.00	0.00	0.00			
	\mathcal{I}_2	0.00 ± 0.00	-0.00 ± 0.00	0.00 ± 0.00			
	\mathcal{I}_3	0.00 ± 0.00	-0.00 ± 0.00	0.00 ± 0.00			
(1,3)	(Analytic)	0.24	0.00	0.24			
	\mathcal{I}_2	0.18 ± 0.00	0.01 ± 0.00	0.19 ± 0.00			
	\mathcal{I}_3	0.19 ± 0.00	0.01 ± 0.00	0.20 ± 0.00			
(2,3)	(Analytic)	0.00	0.00	0.00			
	\mathcal{I}_2	0.00 ± 0.00	0.00 ± 0.00	0.00 ± 0.00			
	\mathcal{I}_3	0.00 ± 0.00	0.00 ± 0.00	0.00 ± 0.00			
(1,2,3)	(Analytic)	0.00	0.00	0.00			
	\mathcal{I}_2	0.00 ± 0.00	-0.00 ± 0.00	0.00 ± 0.00			
	\mathcal{I}_3	0.01 ± 0.00	0.00 ± 0.00	0.01 ± 0.00			

Illustration 2: California housing dataset

We consider the California housing dataset. This dataset has nine variables, eight predictors and a single response variable ‘median house value.’ We standardize all variables to have zero mean and unit variance and utilize an ensemble of GBR’s indexed on

$$\mathcal{I} = \{(i, (1, \dots, 8)) : i \in [3]\},$$

each having 5×10^3 trees, to estimate the HDMR per (16).

Variable importance We conduct a structural and correlative sensitivity analysis (SCSA) and show sensitivity indices with $\epsilon \geq 0.01$ below in Table 5. Latitude and longitude each have strong negative correlative contributions to explained variance and participate in an modest-sized interaction. The relative sensitivity indices R (derived from the total T) are compared to the tree-based feature importance measure. HDMR places more emphasis on ‘MedInc’, ‘Latitude’, and ‘Longitude’ than the tree-based indices.

Table 5: Sensitivity analysis for the California housing dataset, P_ϵ , with $\epsilon = 0.01$

Subspace	Variables	\mathbb{S}^a	\mathbb{S}^b	\mathbb{S}	T	R	Tree
(1,)	(‘MedInc’,)	0.1346	0.1228	0.2574	0.3151	0.2637	0.1240
(2,)	(‘HouseAge’,)	-	-	-	0.0377	0.0315	0.0612
(3,)	(‘AveRooms’,)	0.0305	0.0243	0.0548	0.0966	0.0808	0.1322
(4,)	(‘AveBedrms’,)	-	-	-	0.0310	0.0259	0.0839
(5,)	(‘Population’,)	-	-	-	0.0145	0.0121	0.0803
(6,)	(‘AveOccup’,)	0.0390	0.0168	0.0557	0.1310	0.1096	0.1475
(7,)	(‘Latitude’,)	0.7003	-0.5356	0.1646	0.2880	0.2411	0.1650
(8,)	(‘Longitude’,)	0.6585	-0.5218	0.1367	0.2810	0.2352	0.2058
(2, 6)	(‘HouseAge’, ‘AveOccup’)	0.0069	0.0081	0.0150	-	-	-
(6, 8)	(‘AveOccup’, ‘Longitude’)	0.0066	0.0046	0.0112	-	-	-
(7, 8)	(‘Latitude’, ‘Longitude’)	0.0563	0.0168	0.0732	-	-	-
		1.6374	-0.8562	0.7813	1.1948	1.00	1.00

One-dimensional variable dependence Figures 11 and 22 show HDMR and partial dependence for ‘MedInc’, ‘Latitude’, and ‘Longitude.’ HDMR and partial dependence are similar for ‘MedInc,’ although HDMR generally is smoother. For ‘Latitude’ and ‘Longitude’ they are somewhat different: HDMR profiles are generally vertically shifted to more negative values.

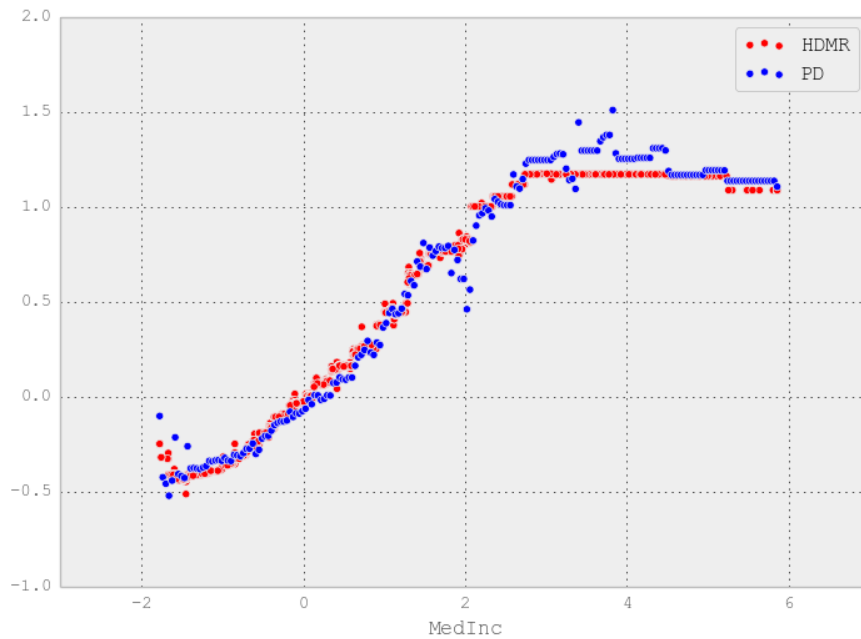


Figure 11: HDMR and partial dependence for ‘MedInc’

Two-dimensional variable dependence In Figure 12 we show the HDMR component function of latitude and longitude. In comparison to partial dependence (Figure 10.17 of Hastie et al. [2009]), HDMR reveals large positive values in scattered eastern localities and reveals positive contributions in northern-most and eastern-most locations.

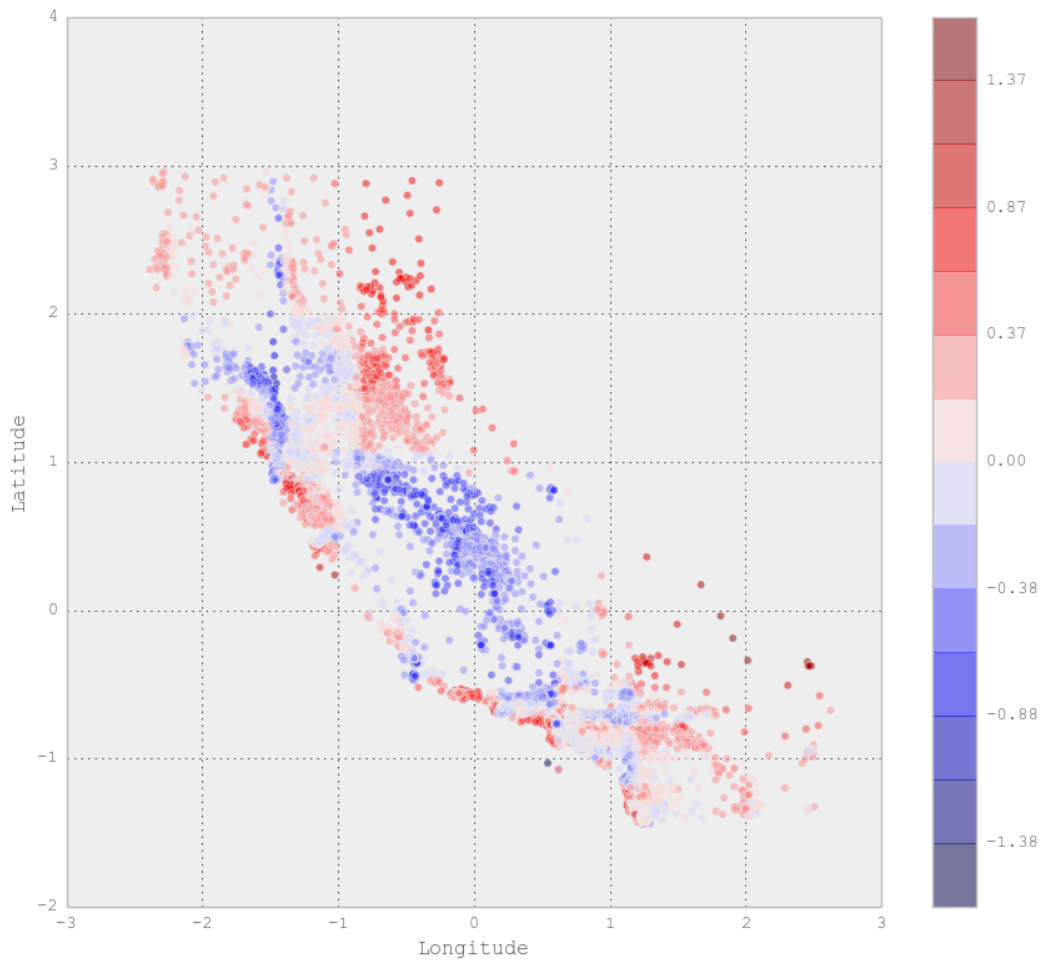


Figure 12: HDMR component function in latitude and longitude

6 Concluding Remarks

HDMR provides structured information on the variable importance and dependence for square-integrable functions. As such, it provides information necessary and sufficient to interpret the model output in terms of the model input and constitutes a glass box representation. This research highlights key utilities of HDMR to supervised machine learning applications and introduces algorithmic constructions from black box models. One is that HDMR can identify sources of information leakage. This is demonstrated for goodness-of-fit settings for “big-data” and popular machine learning interpretative diagnostics and black boxes. Second, HDMR is a useful tool for managing the curse of dimensionality, as it often admits efficient reduced-order representations of dense high-dimensional systems. Third, whenever input variables are correlated, the HDMR component functions are functions of the input distribution parameters including those for correlation. Fourth, HDMR can be applied as a wrapper method for black boxes to provision glass boxes. Collectively, these results suggest HDMR to have broad utility within machine learning.

Acknowledgements

CB acknowledges support for this project from the National Institute of Dental and Craniofacial Research of the National Institutes of Health (NIH-NIDCR Grant No. K08-DE-021430). HR acknowledges support from the National Science Foundation. We thank Grzegorz A. Rempala for comments helpful to improving the article.

Computational implementations

PD (GBR) is computationally implemented using the scikit learn (version 0.18) classes *GradientBoostingRegressor* and *partial-dependence*.

Appendices

χ_n^2 decomposition

Recall the PGOF statistic

$$\chi_n^2 = n \sum_{k \in [k_n]} \frac{(\hat{\mu}_n\{k\} - \mu_n\{k\})^2}{\mu_n\{k\}}$$

with empirical probability $\hat{\mu}_n$ defined as

$$\hat{\mu}_n\{k\} = n^{-1} \sum_{j \in \mathbb{N}_n} I(X_{nj}, k).$$

Put $(x_1, \dots, x_n) \equiv (X_{n1}, \dots, X_{nn})$. Observe that the statistic χ_n^2 is a function of the random observation vector (x_1, \dots, x_n) . In Rempala and Wesolowski [2016] χ_n^2 is decomposed into two uncorrelated components,

$$\chi_n^2 = n^{-1}(S_n + U_n) - n,$$

where

$$S_n = \sum_i \mu_n^{-1}\{x_i\}$$

and

$$U_n = \sum_{\substack{i,j \\ i \neq j}} \mu_n^{-1}\{x_i\} I(x_i, x_j)$$

with

$$\mathbb{E} S_n = n k_n, \quad \mathbb{E} U_n = n(n-1), \quad \mathbb{E} \chi_n^2 = k_n - 1.$$

This gives

$$\mathbb{V}ar \chi_n^2 = n^{-1} (\mathbb{V}ar \mu_n^{-1}\{X_n\} + 2(n-1)(k_n-1)).$$

This is a second-order HDMR,

$$\chi_n^2(x_1, \dots, x_n) = f_0 + \sum_i f_i(x_i) + \sum_{i < j} f_{ij}(x_i, x_j),$$

where

$$\begin{aligned} f_0 &= k_n - 1 \\ f_i(x_i) &= n^{-1} (\mu_n^{-1}\{x_i\} - k_n) \\ f_{ij}(x_i, x_j) &= 2 n^{-1} (\mu_n^{-1}\{x_i\} I(x_i, x_j) - 1), \end{aligned}$$

with

$$\mathbb{V}\text{ar } f_i = n^{-2} \mathbb{V}\text{ar } \mu_n^{-1}\{X_n\}$$

and

$$\mathbb{V}\text{ar } f_{ij} = 4n^{-2}(k_n - 1).$$

Note that if

$$(k_n n)^{-1} \mathbb{V}\text{ar } \mu_n^{-1}\{X_n\} \xrightarrow{n, k_n \rightarrow \infty} 0,$$

then $(2k_n)^{-1/2} \sum_i f_i(x_i) \rightarrow 0$ in probability. This is satisfied for uniform and power law ($\alpha \in [0, 1)$) discrete random variables. Hence, for $k_n \rightarrow \infty$ as $n \rightarrow \infty$, the first-order terms converge to constants and the asymptotic influence of the second-order terms dominates, i.e. the distributional limit of χ_n^2 is determined by the second-order component functions.

This is equivalently stated using the sensitivity indices, $\sum_{i < j} \mathbb{S}_{ij} \xrightarrow{n, k_n \rightarrow \infty} 1$. Putting $n/\sqrt{k_n} \rightarrow \lambda$, it turns out that $\chi_n^2 \xrightarrow{\lambda = \infty}$ Gaussian, $\chi_n^2 \xrightarrow{0 < \lambda < \infty}$ Poisson, and $\chi_n^2 \xrightarrow{\lambda = 0}$ Degenerate. Hence, the distributional limit of χ_n^2 is standard Gaussian for (i) $n, k_n \rightarrow \infty$ with $\lambda = \infty$ or for (ii) $n \rightarrow \infty$ and $k_n = k < \infty$; however, for $n, k_n \rightarrow \infty$ and $\lambda < \infty$ this is not true. Consequently, an improved statistic for χ_n^2 is defined using HDMR,

$$\begin{aligned} \chi_{n\text{HDMR}}^2(x_1, \dots, x_n) &\equiv f_0 + \sum_{i < j} f_{ij}(x_i, x_j) \\ &\equiv \chi_n^2(x) - \sum_i f_i(x_i). \end{aligned}$$

A precise characterization of the asymptotic behavior of χ_n^2 is stated below. Note that this result also holds for power-law distributions.

Theorem 1 (Limit theorem for χ_n^2 for the uniform distribution). *Assume $\mu_n\{x\} = k_n^{-1}$ for $x \in K_n$ and $n = 1, 2, \dots$, as well as*

$$n/\sqrt{k_n} \rightarrow \lambda.$$

Then,

$$\frac{\chi_n^2 - k_n}{\sqrt{2k_n}} \xrightarrow{d} \begin{cases} 0 & \text{when } \lambda = 0 \\ \frac{\sqrt{2}}{\lambda} Z - \frac{\lambda}{\sqrt{2}}, \quad Z \sim \text{Poisson}\left(\frac{\lambda^2}{2}\right) & \text{when } \lambda \in (0, \infty) \\ N \sim \text{Gaussian}(0, 1) & \text{when } \lambda = \infty. \end{cases}$$

Simple product function

For the function $f(x) = \prod_{i=1}^n x_i$, the partition of variance is given by

$$\mathbb{V}\text{ar}(f) = \sigma_f^2 = \sum_i \sigma_i^2 + \sum_{i < j} \sigma_{ij}^2 + \dots + \sigma_{1\dots n}^2,$$

where

$$\sigma_u^2 = \int_{X_u} f_u^2(x_u) d\nu_u(x_u)$$

$$\nu_u(x_u) = \prod_{i \in u} \nu_i(x_i)$$

and

$$\sigma_f^2 = \mu^{2n} ((1 + \rho^2)^n - 1)$$

$$\sigma_i^2 = \mu^{2n} \rho^2$$

$$\sigma_{ij}^2 = \mu^{2n} \rho^4$$

$$\vdots$$

$$\sigma_{i_1 \dots i_k}^2 = \mu^{2n} \rho^{2k}.$$

Figure 13 shows the percent of explained variance of $f^T(x_1, \dots, x_n)$ in (n, T) for $\rho = \frac{1}{2}$. The curves correspond to different values of T , where $(1, \dots, n)$ is left-to-right. As exhibited, increasing T increases the explained variance.

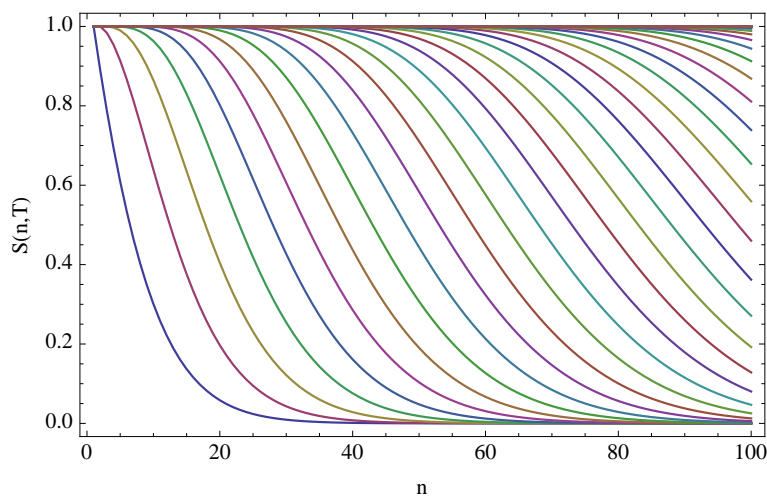


Figure 13: $\mathbb{S}(n, T) = \sum_{k=1}^T p\{k\}$ for $(n, T) \in \{1, \dots, 100\}^2$ and $\rho = \frac{1}{2}$

Figure 14 reveals that the necessary value of T to attain a given percent of explained variance depends upon ρ .

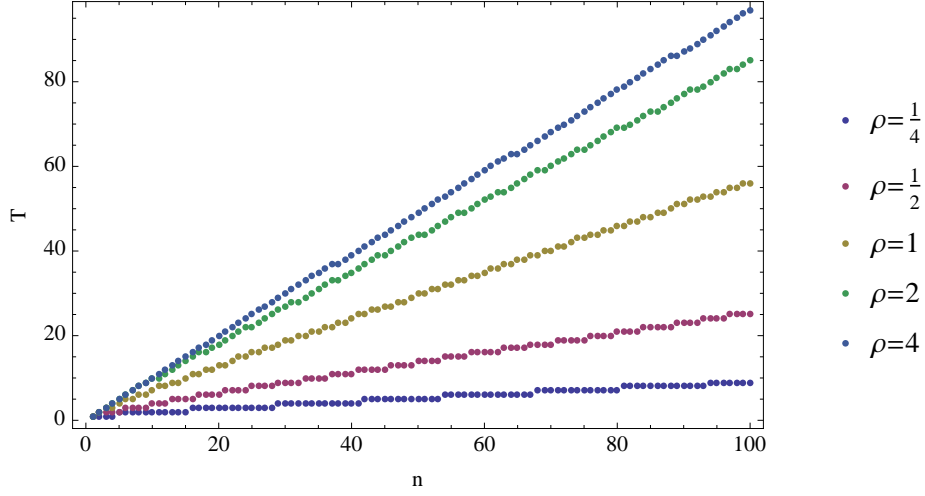


Figure 14: $\min T$ such that $S(n, T) \geq 0.9$ for $(n, \rho) \in \{1, \dots, 100\} \times \{\frac{1}{4}, \frac{1}{2}, 1, 2, 4\}$

Polynomials as linear combinations of monomials

Defining the monomial

$$x_u = \prod_{i \in u} x_i$$

with *iid* x , having common μ and σ^2 , we consider a linear combination of monomials,

$$e_T(\beta, x) = \sum_{\substack{u \\ |u| \leq T}} \beta_u x_u.$$

The variance of e_T is

$$\text{Var}(e_T) = \mathbb{E}[(\sum_{\substack{u \\ |u| \leq T}} \beta_u (x_u - \mu^{|u|}))^2] = \sum_{\substack{u \\ |u| \leq T}} \beta_u^2 \text{Var}(x_u) + 2 \sum_{\substack{u < v \\ |u|, |v| \leq T}} \beta_u \beta_v \text{Cov}(x_u, x_v),$$

where, putting $\rho = \sigma/\mu$,

$$\begin{aligned} \text{Var}(x_u) &= \mu^{2|u|}((1 + \rho^2)^{|u|} - 1). \\ \text{Cov}(x_u, x_v) &= \mu^{|u|+|v|}((1 + \rho^2)^{|u \cap v|} - 1). \end{aligned}$$

$e_T(\beta, x)$ is factorized as

$$\begin{aligned}
e_T(x) &= x_i \left(\sum_{\substack{|u| \leq T-1 \\ |i \cap u|=0}} \beta_{iu} x_u \right) + \left(\sum_{\substack{|u| \leq T \\ |i \cap u|=0}} \beta_u x_u \right) \\
&= x_{ij} \left(\sum_{\substack{|u| \leq T-2 \\ |ij \cap u|=0}} \beta_{iju} x_u \right) + x_i \left(\sum_{\substack{|u| \leq T-1 \\ |ij \cap u|=0}} \beta_{iu} x_u \right) + x_j \left(\sum_{\substack{|u| \leq T-1 \\ |ij \cap u|=0}} \beta_{ju} x_u \right) + \left(\sum_{\substack{|u| \leq T \\ |ij \cap u|=0}} \beta_u x_u \right),
\end{aligned}$$

For $\beta = \mathbf{1}$, we call $e_T(x)$ an elementary symmetric polynomial and can compute its conditional expectations as

$$\begin{aligned}
\mathbb{E}[e_T] &= a_{00} \\
\mathbb{E}[e_T | \mathcal{F}_i] &= a_{11}x_i + a_{10} \\
\mathbb{E}[e_T | \mathcal{F}_{ij}] &= a_{22}x_{ij} + a_{21}(x_i + x_j) + a_{20} \\
&\vdots \\
\mathbb{E}[e_T | \mathcal{F}_u] &= \sum_{w \subseteq u} a_{|u||w|} x_w,
\end{aligned}$$

where

$$a_{rs} = \sum_{\substack{|u| \leq T-s \\ |r \cap u|=0}} \beta_{ru} \mu^{|u|} = \sum_{k \leq T-s} \binom{n-r}{k} \mu^k.$$

The component functions of $e_T(x)$ are defined recursively,

$$\begin{aligned}
f_0 &= \mathbb{E}[e_T] \\
f_i(x_i) &= \mathbb{E}[e_T | \mathcal{F}_i] - f_0 \\
f_{ij}(x_i, x_j) &= \mathbb{E}[e_T | \mathcal{F}_{ij}] - f_i(x_i) - f_j(x_j) - f_0 \\
&\vdots \\
f_u(x_u) &= \mathbb{E}[e_T | \mathcal{F}_u] - \sum_{w \subset u} f_w(x_w).
\end{aligned}$$

For $T = n$, we have

$$\sigma_f^2 = (\mu + 1)^{2n} ((\tau^2 + 1)^n - 1)$$

$$f_u(x_u) = (1 + \mu)^{n-|u|} \prod_{i \in u} (x_i - \mu)$$

$$\sigma_u^2 = \tau^{2|u|} (\mu + 1)^{2n}$$

$$q\{k\} = \sum_{i_1 < \dots < i_k} \mathbb{S}_{i_1 \dots i_k} = \frac{\binom{n}{k} \tau^{2k}}{(\tau^2 + 1)^n - 1}$$

where

$$\tau = \frac{\sigma}{\mu + 1} = \frac{\rho}{1 + \frac{1}{\mu}}.$$

When $\tau < 1$, $q\{k\} > p\{k\}$ for $k \ll n$. For the uniform distribution on the unit interval, we have $\tau = \frac{1}{3\sqrt{3}} \approx 0.19$. Furthermore,

$$\lim_{\substack{\mu, \sigma \rightarrow \infty \\ \sigma/\mu = \rho}} \tau = \rho.$$

$$\rho = \frac{1}{2}$$

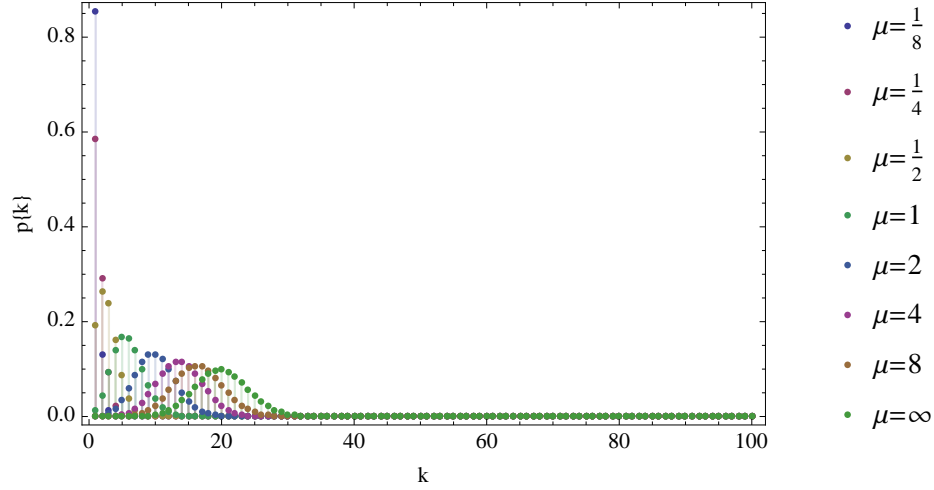


Figure 15: $q\{k\} = \sum_{i_1 < \dots < i_k} \mathbb{S}_{i_1 \dots i_k}$ for $\rho = \frac{1}{2}$

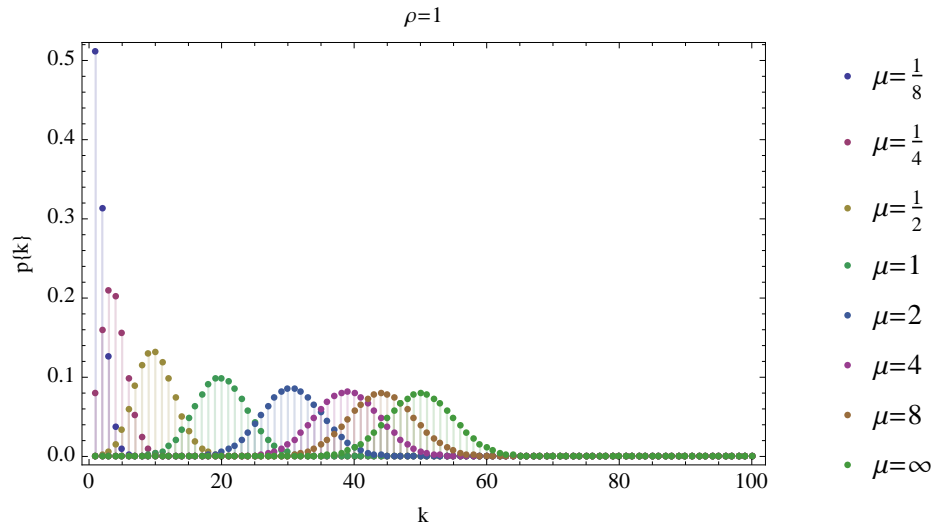


Figure 16: $q\{k\} = \sum_{i_1 < \dots < i_k} \mathbb{S}_{i_1 \dots i_k}$ for $\rho = 1$

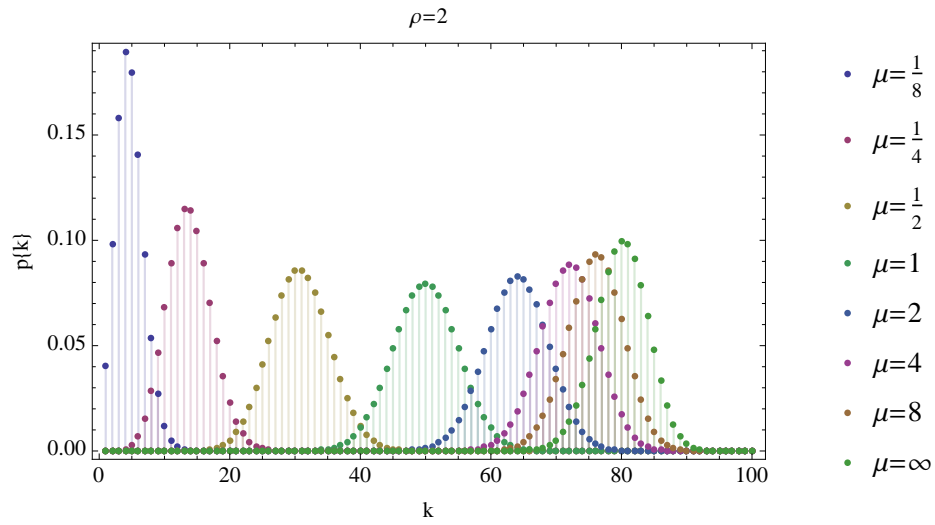


Figure 17: $q\{k\} = \sum_{i_1 < \dots < i_k} \mathbb{S}_{i_1 \dots i_k}$ for $\rho = 2$

Feature vector construction for hierarchically-orthogonal subspaces

Suppose for the measure space $(X_u, \mathcal{X}_u, \mu_u)$ of subspace $u \subseteq \{1, \dots, n\}$, where $\mu_u(x_u) = \int_{X-u} \mu(x_u, dx_{-u})$, we have a collection of basis vectors indexed on $\mathcal{O}(u)$ and having dimensions $b = (b_v \in \mathbb{N} : v \in \mathcal{O}(u))$. This is denoted by

$$\mathbf{B} \equiv \{\mathbf{B}_v \equiv (\mathbf{B}_{v1}, \dots, \mathbf{B}_{vb_v}) : v \in \mathcal{O}(u)\}.$$

We can construct a non-orthogonal basis vector Φ_u having dimension b_u whose elements are hierarchically-orthogonal with respect to μ (and μ_u). To do this, we order $\mathcal{O}(u)$ in size and use the Gram-Schmidt process to generate $\mathbf{Q} = (\mathbf{Q}_v \equiv (\mathbf{Q}_{v1}, \dots, \mathbf{Q}_{vb_v}) : v \in \mathcal{O}(u))$ from \mathbf{B} . If the bases are given on an empirical measure as column vectors of data $\mathbf{B} \in \mathbb{R}^{N \times \text{sum}(b)}$, then QR decomposition is conducted on \mathbf{B} , returning \mathbf{Q} . Then we put $\Phi_u = \mathbf{Q}_u$. Empirically, this is $\Phi_u \in \mathbb{R}^{N \times b_u}$. Repeating this process for all subspaces of interest α we form the feature vector

$$\Phi = \Phi_\emptyset \parallel \Phi_{\{1\}} \parallel \dots \parallel \Phi_{\{n\}} \parallel \Phi_{\{1,2\}} \parallel \dots = \prod_{\alpha \in \alpha} \Phi_\alpha.$$

Putting

$$\Phi \gamma = f,$$

the coefficients are given as

$$\gamma = (\gamma_\alpha : \alpha \in \alpha) = (\Phi \otimes \Phi)^{-1} (\Phi \otimes f).$$

These outer products can be calculated exactly, as they are computations of moments of μ . The component functions are given by

$$f_u(x_u) = \langle \gamma_u, \Phi_u(x_u) \rangle_{\ell^2}.$$

Correlated expansion

A non-orthogonal HDMR basis $\{\Phi_0, \Phi_1, \Phi_2, \Phi_{12}\}$ is formed as

$$\begin{aligned} \Phi_0 &= (1) \\ \Phi_i &= \left(\frac{x_i - \mu_i}{\sigma_i}, \frac{(x_i - \mu_i)^2}{\sigma_i^2} - \sqrt{2} \right), \quad i = 1, 2 \\ \Phi_{12} &= \left(\frac{-\rho\sigma_2^2((\rho^2 - 1)\sigma_1^2 + (x_1 - \mu_1)^2) + (\rho^2 + 1)\sigma_1\sigma_2(x_1 - \mu_1)(x_2 - \mu_2) + \rho\sigma_1^2(-(x_2 - \mu_2)^2)}{(\rho^2 + 1)\sqrt{\rho^2 + \frac{4}{\rho^2 + 1} - 3\sigma_1^2\sigma_2^2}} \right). \end{aligned}$$

The coefficients are given by

$$\begin{aligned}\gamma_0 &= (\beta_0 + \beta_1\mu_1 + \beta_2\mu_2 + \beta_{12}\mu_1\mu_2 + \beta_{12}\rho\sigma_1\sigma_2) \\ \gamma_1 &= \left(\sigma_1(\beta_1 + \beta_{12}\mu_2), \frac{\sqrt{2}\beta_{12}\rho\sigma_1\sigma_2}{\rho^2 + 1} \right) \\ \gamma_2 &= \left(\sigma_2(\beta_2 + \beta_{12}\mu_1), \frac{\sqrt{2}\beta_{12}\rho\sigma_1\sigma_2}{\rho^2 + 1} \right) \\ \gamma_{12} &= \left(\beta_{12}\sqrt{\rho^2 + \frac{4}{\rho^2 + 1}} - 3\sigma_1\sigma_2 \right)\end{aligned}$$

Analytic test function

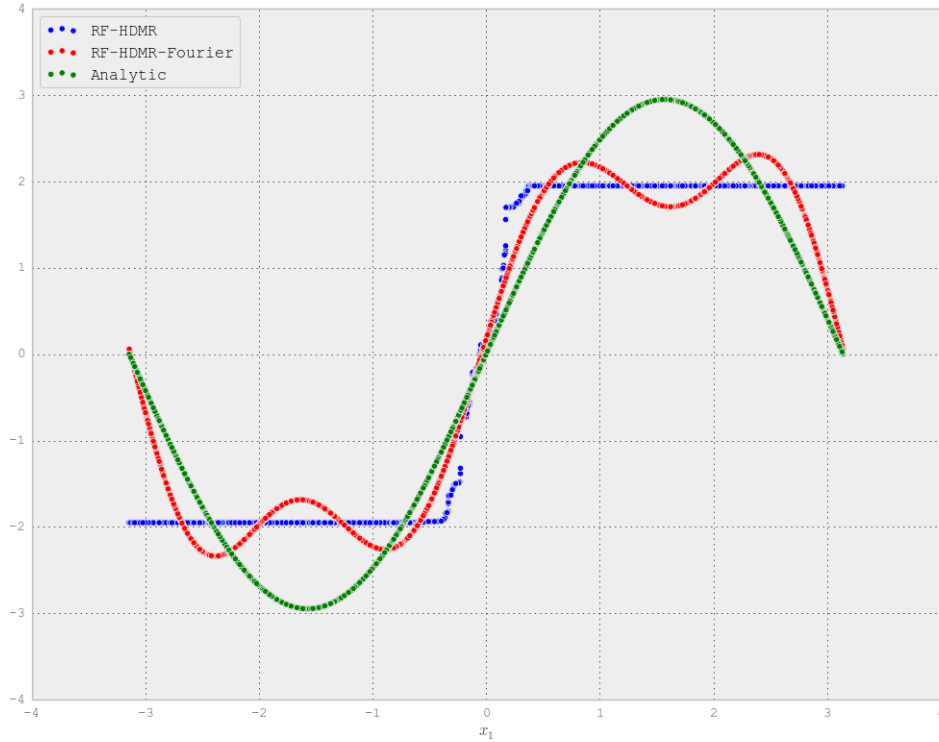


Figure 18: $f_1^{\text{HDMR}}(x_1)$ by RF approximation, smooth Fourier projection, and analytic

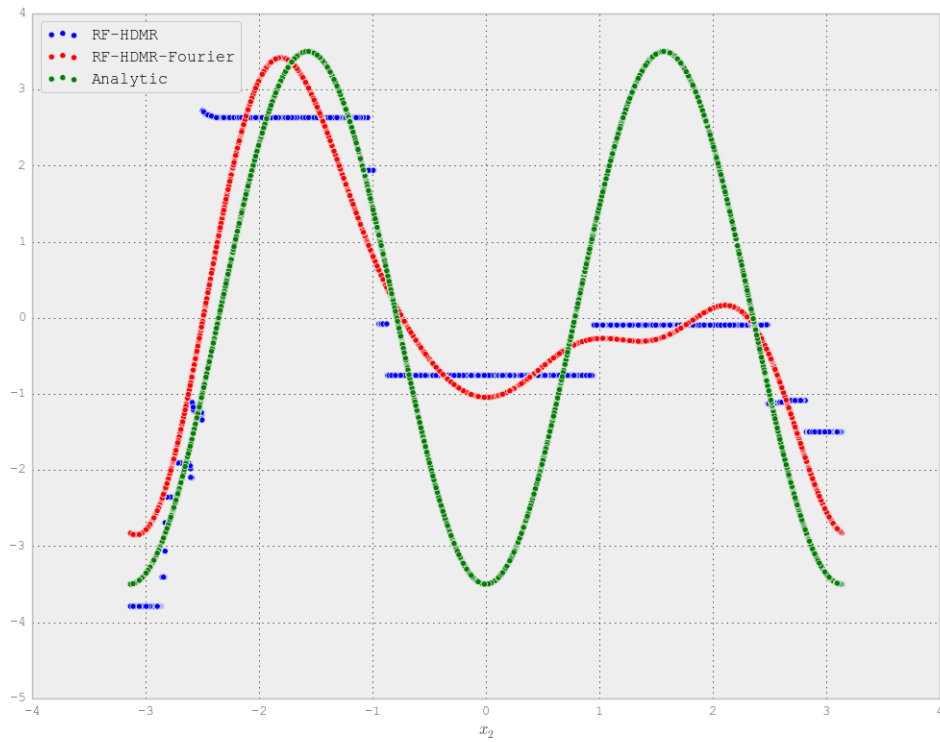
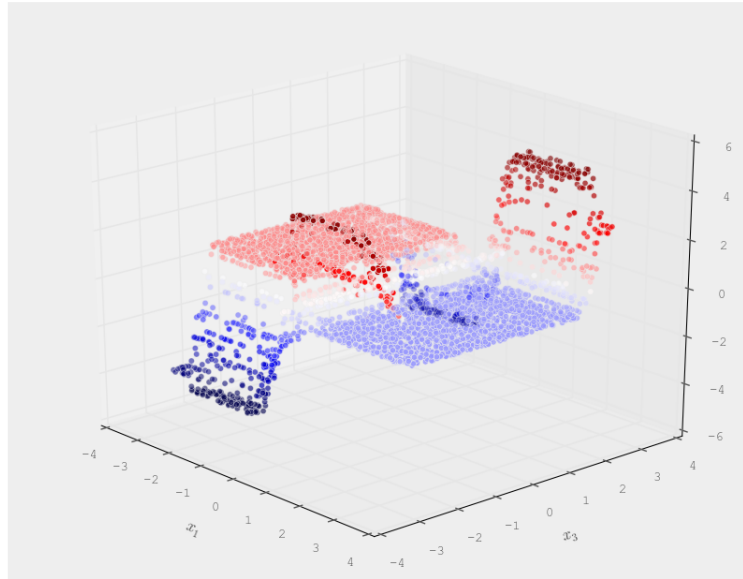


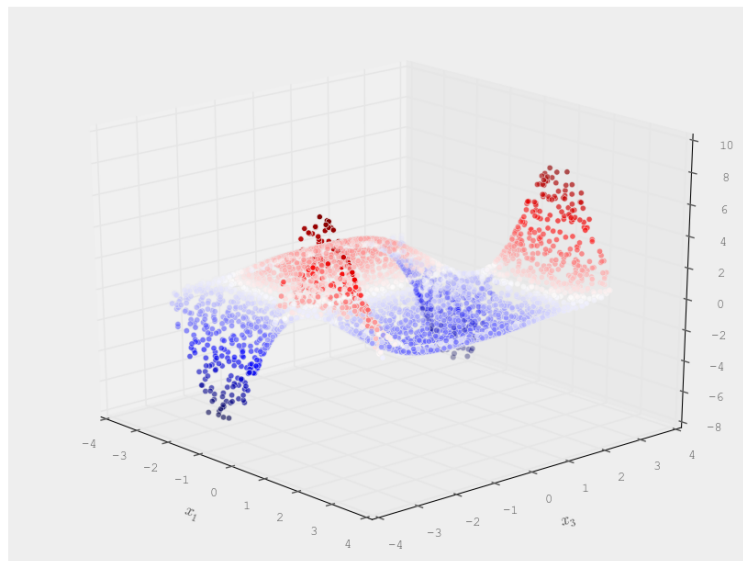
Figure 19: $f_2^{\text{HDMR}}(x_2)$ by RF approximation, smooth Fourier projection, and analytic

Figure 20: $f_{13}^{\text{HDMR}}(x_1, x_3)$ by RF approximation

(a) Decision tree approximation



(b) Analytic



California housing dataset

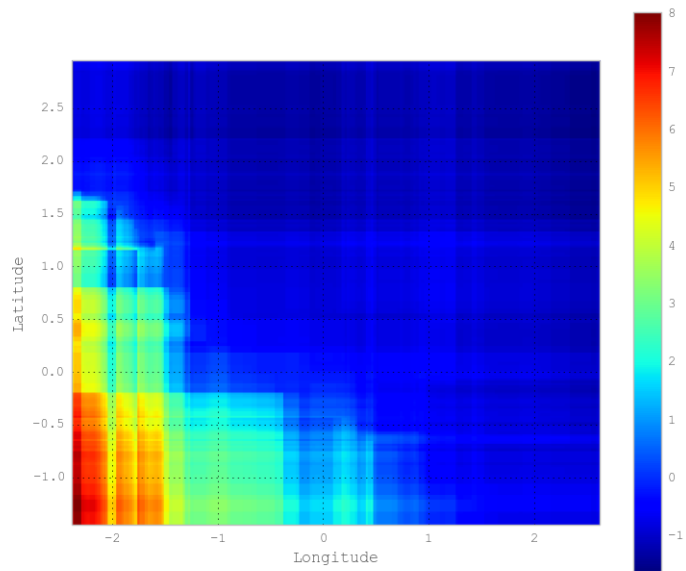


Figure 21: Partial dependence in latitude and longitude as computed by sklearn classes *GradientBoostingRegressor* and *partial-dependence*

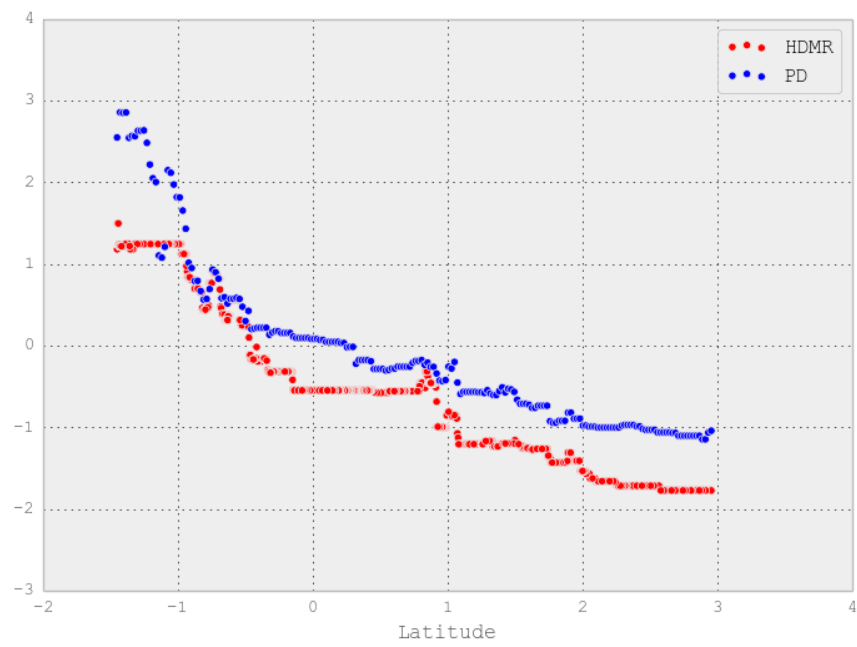


Figure 22: HDMR and partial dependence for 'Latitude'

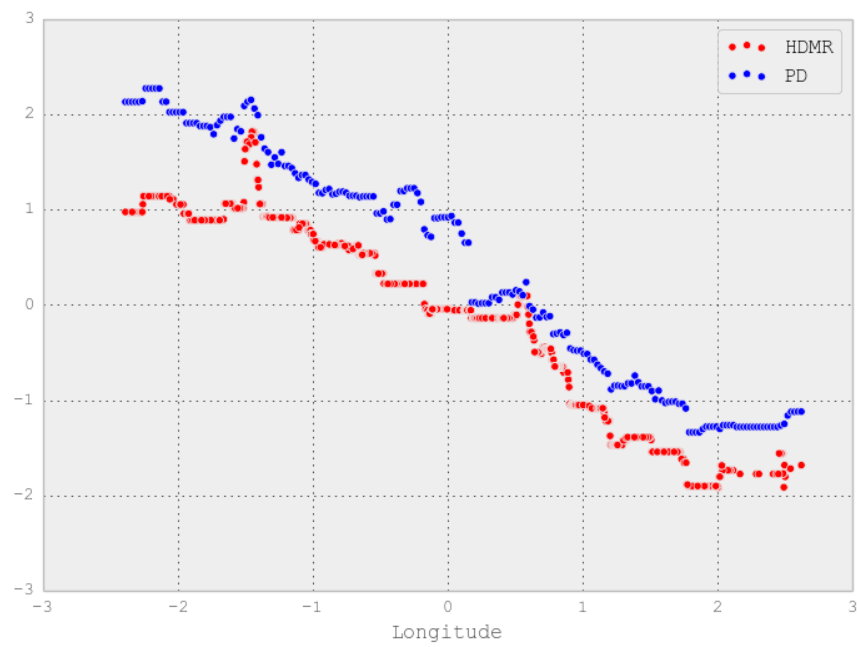


Figure 23: HDMR and partial dependence for ‘Longitude’

References

- Sanjay R. Arwade, Mohammadreza Moradi, and Arghavan Louhghalam. Variance decomposition and global sensitivity for structural systems. *Engineering Structures*, 32(1):1 – 10, 2010. ISSN 0141-0296. doi: <http://dx.doi.org/10.1016/j.engstruct.2009.08.011>. URL <http://www.sciencedirect.com/science/article/pii/S0141029609002788>.
- Leo Breiman. Random forests. *Machine Learning*, 45(1):5–32, 2001. ISSN 1573-0565. doi: 10.1023/A:1010933404324. URL <http://dx.doi.org/10.1023/A:1010933404324>.
- Gaëlle Chastaing, Fabrice Gamboa, and Clémentine Prieur. Generalized hoeffding-sobol decomposition for dependent variables - application to sensitivity analysis. *Electron. J. Statist.*, 6:2420–2448, 2012. doi: 10.1214/12-EJS749. URL <http://dx.doi.org/10.1214/12-EJS749>.
- N. Durrande, D. Ginsbourger, O. Roustant, and L. Carraro. {ANOVA} kernels and {RKHS} of zero mean functions for model-based sensitivity analysis. *Journal of Multivariate Analysis*, 115:57 – 67, 2013. ISSN 0047-259X. doi: <http://dx.doi.org/10.1016/j.jmva.2012.08.016>. URL <http://www.sciencedirect.com/science/article/pii/S0047259X1200214X>.
- Sir Fisher, Ronald Aylmer. On the "probable error" of a coefficient of correlation deduced from a small sample. *Metron*, 1(4):3–32, 1921.
- Jerome H. Friedman. Greedy function approximation: A gradient boosting machine. *Ann. Statist.*, 29(5):1189–1232, 10 2001. doi: 10.1214/aos/1013203451. URL <http://dx.doi.org/10.1214/aos/1013203451>.
- Isabelle Guyon and André Elisseeff. An introduction to variable and feature selection. *J. Mach. Learn. Res.*, 3:1157–1182, March 2003. ISSN 1532-4435. URL <http://dl.acm.org/citation.cfm?id=944919.944968>.
- Jaroslav Hajek. Asymptotic normality of simple linear rank statistics under alternatives. *Ann. Math. Statist.*, 39(2):325–346, 04 1968. doi: 10.1214/aoms/1177698394. URL <http://dx.doi.org/10.1214/aoms/1177698394>.
- Trevor J. Hastie, Robert John Tibshirani, and Jerome H. Friedman. *The elements of statistical learning : data mining, inference, and prediction*. Springer series in statistics. Springer, New York, 2009. ISBN 978-0-387-84857-0. URL <http://opac.inria.fr/record=b1127878>. Autres impressions : 2011 (corr.), 2013 (7e corr.).
- Wassily Hoeffding. A class of statistics with asymptotically normal distribution. *Ann. Math. Statist.*, 19(3):293–325, 09 1948. doi: 10.1214/aoms/1177730196. URL <http://dx.doi.org/10.1214/aoms/1177730196>.

- Giles Hooker. Generalized functional anova diagnostics for high-dimensional functions of dependent variables. *Journal of Computational and Graphical Statistics*, 16(3): 709–732, 2007. doi: 10.1198/106186007X237892. URL <http://dx.doi.org/10.1198/106186007X237892>.
- S.S. Kucherenko I.M. Sobol. On global sensitivity analysis of quasi-monte carlo algorithms. *Monte Carlo Methods and Applications*, 11:83–92, 2004.
- Genyuan Li and Herschel Rabitz. General formulation of hdmr component functions with independent and correlated variables. *Journal of Mathematical Chemistry*, 50(1):99–130, 2012. ISSN 0259-9791. doi: 10.1007/s10910-011-9898-0. URL <http://dx.doi.org/10.1007/s10910-011-9898-0>.
- Genyuan Li and Herschel Rabitz. Analytical hdmr formulas for functions expressed as quadratic polynomials with a multivariate normal distribution. *Journal of Mathematical Chemistry*, 52(8):2052–2073, 2014. ISSN 1572-8897. doi: 10.1007/s10910-014-0365-6. URL <http://dx.doi.org/10.1007/s10910-014-0365-6>.
- G.G. Lorentz, M.V. Golitschek, and Y. Makovoz. *Constructive Approximation*. Springer, New York, 1996.
- Herschel Rabitz and Omer F. Alis. General foundations of high-dimensional model representations. *Journal of Mathematical Chemistry*, 25(2-3):197–233, 1999. ISSN 0259-9791. doi: 10.1023/A:1019188517934. URL <http://dx.doi.org/10.1023/A3A1019188517934>.
- Grzegorz A. Rempala and Jacek Wesolowski. Double asymptotics for the chi-square statistic. *Statistics & Probability Letters*, 119:317–325, 12 2016. doi: <http://dx.doi.org/10.1016/j.spl.2016.09.004>. URL <http://www.sciencedirect.com/science/article/pii/S0167715216301699>.
- I. M. Sobol. On sensitivity estimation for nonlinear mathematical models. *Matem. Mod.*, 2(1):112–118, 1990.
- I. M. Sobol’ and S. Kucherenko. Derivative based global sensitivity measures and their link with global sensitivity indices. *Mathematics and Computers in Simulation*, 79(10): 3009–3017, 6 2009. doi: <http://dx.doi.org/10.1016/j.matcom.2009.01.023>. URL <http://www.sciencedirect.com/science/article/pii/S0378475409000354>.
- I.M. Sobol. Global sensitivity indices for nonlinear mathematical models and their monte carlo estimates. *Mathematics and Computers in Simulation*, 55(1-3):271–280, 2001.
- Carolin Strobl, Anne-Laure Boulesteix, Achim Zeileis, and Torsten Hothorn. Bias in random forest variable importance measures: Illustrations, sources and a solution. *BMC*

Bioinformatics, 8(1):25, 2007. ISSN 1471-2105. doi: 10.1186/1471-2105-8-25. URL <http://dx.doi.org/10.1186/1471-2105-8-25>.

Akimichi Takemura. Tensor analysis of ANOVA decomposition. 78(384):894–900, 1983. ISSN 0162-1459 (print), 1537-274X (electronic).

Vladimir N. Vapnik. *The Nature of Statistical Learning Theory*. Springer-Verlag New York, Inc., New York, NY, USA, 1995. ISBN 0-387-94559-8.

G. Wahba. *Spline Models for Observational Data*. Society for Industrial and Applied Mathematics, 1990. doi: 10.1137/1.9781611970128. URL <http://epubs.siam.org/doi/abs/10.1137/1.9781611970128>.

Grace Wahba, Yuedong Wang, Chong Gu, Ronald Klein, and Barbara Klein. Smoothing spline anova for exponential families, with application to the wisconsin epidemiological study of diabetic retinopathy. *The Annals of Statistics*, 23(6):1865–1895, 1995. URL <http://www.jstor.org/stable/2242776>.